PERTURBATIONS TO THE ALLOSTERIC REGULATION OF CARBAMOYL PHOSPHATE SYNTHETASE UPON REMOVAL OF INTERFACIAL RESTRAINTS

A Dissertation

by

ROBERT ELI KOENIG

Submitted to the Office of Graduate and Professional Studies of
Texas A&M University
in partial fulfillment of the requirements for the degree of

DOCTOR OF PHILOSOPHY

Chair of Committee,	Gregory D. Reinhart
Committee Members,	Frank M. Raushel
	Paul D. Straight
	Hays S. Rye
Head of Department,	Gregory D. Reinhart

December 2017

Major Subject: Biochemistry

ABSTRACT

Carbamoyl phosphate synthetase (CPS) from *E. coli* is an αβ heterodimeric allosterically regulated enzyme serving as a gatekeeper for entry into both the de novo pyrimidine biosynthesis pathway and the urea cycle (in ureotelic organisms). The regulation of CPS by the activator L-ornithine and inhibitor UMP is an entropy dominated phenomenon. Liberation of the heterodimeric interface by removal of the glutaminase subunit creates increased conformational freedom at the interface and maintains the functionality of the two reaction centers located in the large subunit. The liberation of the interface has profound effects on the allosteric regulation of the two reaction centers and causes a perturbation in the mechanism of the ATP synthesis reaction when investigated with steady state kinetics.

Van't Hoff analysis of Q_{ax}, the coupling parameter, demonstrated ornithine binding generates a decrease in ΔG_{ax}, the coupling free energy, of the bicarbonate dependent ATPase reaction of 1.1 kcal/mol in the absence of the glutaminase subunit indicating an augmentation of ornithine's ability to activate CPS from *E. coli*. The loss of the glutaminase subunit results in the ΔG_{ax} of activation of the ATP synthesis reaction being increased by 0.8 kcal/mol resulting in attenuation of activation. Quantification of Q_{ay} and determination of ΔG_{ay} of inhibition by UMP demonstrated inhibition of MgATP binding by UMP is also augmented in the absence of the glutaminase subunit, with an increase of 0.44 kcal/mol while data suggests the inhibition of the ATP synthesis reaction is abolished upon removal of the glutaminase subunit.

Consequently, releasing the structural restraints imposed by a subunit interaction with no catalytic constraints can have substantial, though unpredictable effects on allosteric communication in *E. coli* CPS.

DEDICATION

Dedicated to my dad, who always told me to keep asking why.

ACKNOWLEDGEMENTS

I would like to thank Dr. Reinhart, my advisor, for all the hard work he put into me as a scientist. It is never easy teaching an old dog new tricks. Thanks for doing so. To my advisory committee: Dr. Raushel, Dr. Straight and, Dr. Rye, thank you for the years of advice, suggestions and, help throughout this journey.

Thank you to the biochemistry department staff, without you this department would fall apart around our heads. Also, my fellow students, past and present, your collaboration, friendship and shared suffering has given me the strength to finish.

Most importantly I want to thank my family. They are always present to lend an ear even if they have no clue what I'm talking about. A special thank you to my wife to be, Amanda, you are the reason I strive to be a better man. You make me push myself to new heights. Thank you. Thank you all for your support and help.

CONTRIBUTORS AND FUNDING SOURCES

This work was supervised by a dissertation committee consisting of Professor Gregory Reinhart, Professor Paul Straight, and Professor Hays Rye of the Department of Biochemistry and Biophysics and Professor Frank Raushel of the Department of Chemistry. All work for the dissertation was completed independently by the student.

This work was made possible in part by National Institutes of Health under grant number R01 GM 033216, The Welch Foundation under grant number A-1543 and support from Texas A&M Agrilife Research. Its contents are solely the responsibility of the authors and do not necessarily represent the official views of the supporting agencies.

NOMENCLATURE

BPG	2,3-Bisphosphoglycerate
CP	Carbamoyl phosphate
CPS	Carbamoyl phosphate Synthetase
CTP	Cytidine Triphosphate
DTT	Dithiothreitol
EDTA	Ethylenediaminetetraacetic acid
$FADH_2$	Flavin Adenine Dinuclueotide
F1-6BP	Fructose-1,6 Bisphosphate
F6P	Fructose-6-Phosphate
HEPES	4-(2-hydroxyethyl)-1-piperazineethanesulfonic acid
IMP	Inosine Monophosphate
MgADP	Magnesium Adenosine Monophosphate
MgATP	Magnesium Adenosine Triphosphate
NADH	Nicotinamide Adenine Dinucleotide
PEP	Phospho(enol) Pyruvate
PFK	Phosphofructokinase
UMP	Uridine Monophosphate

TABLE OF CONTENTS

Page

LIST OF FIGURES

Page

LIST OF TABLES

Page

CHAPTER I

INTRODUCTION

Allostery in Metabolism and Drug Design

There are many types of regulation, ranging from governmental regulation of international commerce to the regulation of quantum spin states by the laws of physics. One form of regulation in the realm of biochemical and biophysical investigations is the regulation of proteins and enzymes. Even in the much narrower area containing protein regulation, there are still many ways to reach the objective. A cell can regulate the level of transcription of a gene coding for a specific protein, or it can regulate the translation of the mRNA. After a protein is translated, there are further layers of regulation at the cell's disposal, e.g., post-translational covalent modifications, that can serve as both activators and inhibitors of protein activity. Finally, once a protein is mature and active, another level of regulation can be evoked. Substrate or non-substrate ligands can also regulate protein function by affecting binding events that cause a change in either the affinity for substrate or a change in the turnover of the catalytically competent complex. With further refinement of the definition of enzyme regulation, one can discuss allosteric regulation. The idea that a small molecule binds to a protein and affects function was first proposed by Linus Pauling, and the term allostery was later coined by Monod, Wyman, and Chengeaux[1,2]. The allosteric regulation of an enzyme is defined as the alteration of affinity for a ligand or catalytic activity as a function of ligand binding at a distinct site that is separated in space from the site of the alteration.

Several enzymes and proteins are regulated by allosteric ligands. The earliest, and in all probability, the most studied protein is hemoglobin. Work with purified hemoglobin in the early 20th century began to untangle the mysteries of how oxygen binds to the heme moiety and how the interactions between heme groups affect the affinity for molecular oxygen. The change in affinity for oxygen induced by ligands was of particular interest, because they have no stereochemical similarity to oxygen, suggesting alternative binding sites. Protons (H^+), CO_2, and 2,3-bisphosphoglycerate (BPG) all serve to reduce the binding affinity of mammalian hemoglobins for molecular oxygen[3]. The occurrence of allosteric inhibition was suggested because it was likely that ligands did not bind the same location as molecular oxygen on hemoglobin; therefore, they were not competitively inhibiting oxygen binding. All three of these ligands do indeed bind to distinct sites from molecular oxygen[4].

The Bohr effect, proposed by Christian Bohr, reports on the allosteric effect that protons (H^+) have on hemoglobin's affinity for oxygen. In the $\alpha_2\beta_2$ structure of tetrameric hemoglobin, there are several inter- and intra-subunit salt bridges. The most notable are the interactions within the beta subunits (Arg94 and His146) and the alpha subunits (Arg141 and Asp126). The deprotonated state of His146 is found in the oxygenated hemoglobin, so as the pH decreases, the concentration of protons increases. The resulting increase in protons causes protonation of side chain residues in hemoglobin, shifting the conformational population to favor a lower affinity conformational state. On the alpha subunit Asp126 is also deprotonated when hemoglobin is oxygenated. Through the same shift in the conformation population, the

protonation of Asp126 on the alpha subunit results in decreased affinity for molecular oxygen. Since the protonated residues are not directly involved in the binding of oxygen, protons allosterically inhibit oxygen binding to hemoglobin.

Carbon dioxide is a by-product of energy production in living organisms that utilize oxidative phosphorylation[5]. Carbon dioxide is generated when pyruvate is processed through the citric acid cycle or lactic acid is generated by the reduction of pyruvate in anaerobic fermentation in higher organisms. Carbon dioxide can be toxic and must be removed from the system. When present, hemoglobin serves as a transport protein for excess CO_2 by forming carbamates at the amino termini of the alpha subunits. The carbamation of the amino termini again causes a shift in the population of conformations to favor the lower binding affinity. The ligation of CO_2 with a site distinctive from the heme group, which affects the affinity for oxygen, demonstrates the allosteric nature of CO_2 on oxygen binding.

2,3-bisphosphoglycerate (BPG) is a small biological molecule found in erythrocytes that acts as another allosteric inhibitor in hemoglobin. BPG binds to the central cavity of hemoglobin, where the phosphate groups are coordinated by His143 from each beta chain and His2 from each alpha chain[3]. These interactions between BPG and residues in all four subunits essentially prevent conformational shifts induced when oxygen binds the heme moiety. BPG stabilizes the deoxygenated form, decreasing the affinity for oxygen while bound at a distinct binding site.

Hemoglobin is an outstanding example of a protein exhibiting allosteric regulation. However, more importantly, enzymes are also regulated by allosteric ligands.

Phosphofructokinase (PFK) is the enzyme that catalyzes the first committed step of glycolysis. Prokaryotic PFK has been extensively studied, and the allosteric response is well established[6–10]. Allosteric regulation in PFK is accomplished by a precise balance between the primary inhibitor, phospho-enol-pyruvate (PEP), and the activating ligand, adenosine 5'-diphosphate (ADP). Both PEP and ADP bind to a site that is physically removed from the catalytic site of PFK and regulate the affinity of PFK for the substrates MgATP and fructose-6-phosphate (F6P).

PFK, which is found in prokaryotic organisms, is a homotetramer and a dimer of dimers. The quaternary organization of the two dimers generates an interesting set of binding sites for both substrates and allosteric effectors. As observed in Figure 1, one dimer interface forms the binding pocket for the substrates (F-1,6-BP, green), and the interface between the dimers generates the allosteric ligand pocket (MgADP, red)[11]. The allosteric binding sites in prokaryotic PFK are capable of accommodating both activating ADP and inhibiting PEP.

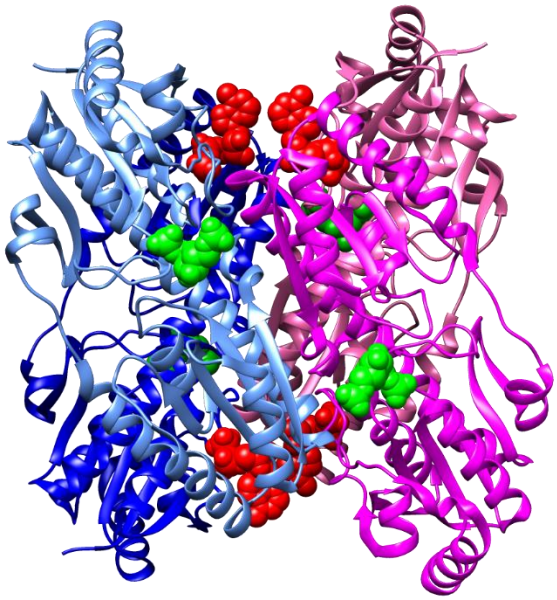

Figure 1: Tetrameric construct of PFK illustrating fructose-1,6-bisphosphate (green) in the active site and MgADP (Red) in the allosteric site. Modeled from PDID: 1PFK[12].

Studies of PFK and hemoglobin have provided great insight into the complex nature of allosteric regulation in macromolecules; however, there are larger implications of the allosteric regulation of enzymes in metabolic pathways. The elucidation of glycolytic intermediates and reactions won Otto Meyerhof the Nobel Prize in Medicine in 1922, and his contemporary, Gustav Embden, received twelve nominations for the Nobel Prize but never won it. The pathway to which they contributed so much now bears their name, the Embden–Meyerhof pathway.

Understanding glycolysis has direct implications on the metabolism of organisms that make use of glucose to produce cellular energy via oxidative phosphorylation. The end product of glycolysis, pyruvate, enters the Krebs's cycle to produce the reduced cofactors NADH and $FADH_2$, and as such, the regulation of glycolysis is important for an organism's viability. Glycolysis is predominantly regulated at the reaction catalyzed by PFK, which commits F6P to its glycolytic fate. However, the pathway is also regulated at the final reaction of glycolysis, catalyzed by pyruvate kinase; pyruvate can be siphoned off for other metabolic processes.

Pyruvate, the end product of glycolysis, does not exclusively feed into the Krebs's cycle. The versatility of pyruvate as a precursor for the synthesis of several amino acids and as a substrate for anaerobic fermentation, makes it an important branch point for many metabolic pathways. Unsurprisingly, the regulation of pyruvate kinase is carried out on several levels. On a systemic level , the hormone glucagon causes a doubling of the $K_{1/2}$ of PEP in isolated rat hepatocytes from 170 to 370 μM[13]. Allosteric regulators of pyruvate kinase include L-alanine, an immediate product of the amination

of pyruvate, and F-1,6-BP, an indicator of increased glycolytic flux[13,14]. L-alanine is formed from pyruvate in one step via the transfer of the amino group of glutamate to pyruvate, resulting in α-ketoglutarate, and it provides a checkpoint for alanine biosynthesis. The R, L, and M2 isozymes of pyruvate kinase found in mice and human tumors are inhibited by L-alanine[14–17]. F-1,6-BP, the product of the reaction catalyzed by PFK, stimulates the activity of pyruvate kinase[18]. In pyruvate kinase isolated from *Saccharomyces cerevisiae* the binding site for F-1,6-BP is located 40 Å distal to the active site, and binding induces a dramatic conformational change in the tertiary structure. The shift in conformation activates pyruvate kinase by increasing affinity for PEP and ensuring that there is not a buildup of glycolytic intermediates.

Glycolysis is not the only pathway containing enzymes that are allosterically regulated. Both the urea cycle and pyrimidine nucleotide biosynthesis are allosterically regulated at key checkpoints. The synthesis of *de novo* pyrimidine nucleotides is a multistep pathway that combines Carbamoyl phosphate and L-aspartate to form the pyrimidine ring, followed by phosphoribosylation of the pyrimidine. Then, the substituents on the ring are modified to generate the specific pyrimidine nucleotides (Figure 2).

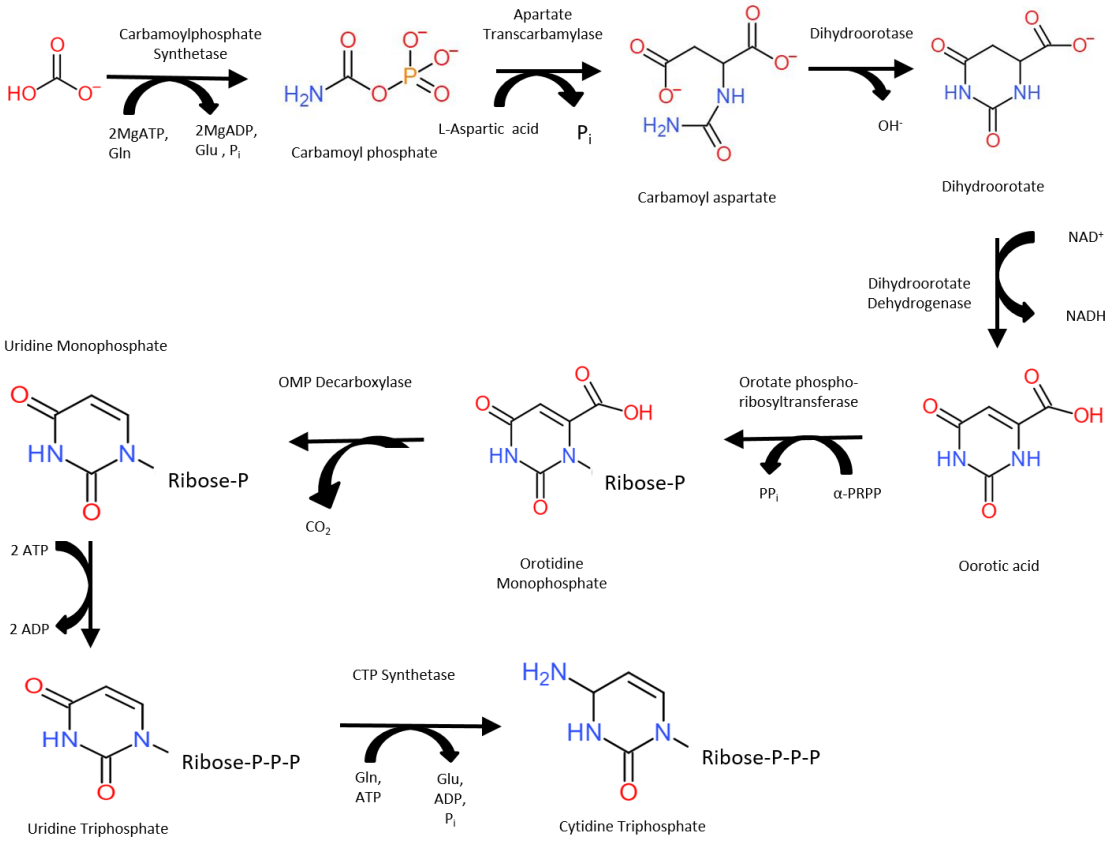

Figure 2: Steps of pyrimidine biosynthesis. Initial allosteric regulation by UMP occurs at CPS, followed by allosteric regulation of CTP synthetase by CTP.

Pyrimidine nucleotide synthesis has two key checkpoints in the metabolic pathway. CPS regulates entry into the pathway by generating one of the precursors, carbamoyl phosphate. The second regulatory enzyme is found after the formation of uridine monophosphate (UMP); the enzyme cytidine triphosphate (CTP) synthetase is regulated to ensure the proper balance of pyrimidine nucleotides in the cell.

CTP synthetase catalyzes the final reaction of pyrimidine biosynthesis and, as mentioned, maintains the balance of UMP and CTP pools in the cell. In prokaryotes, CTP synthetase is inhibited by its product CTP[19]. CPS, on the other hand, serves as the

gatekeeper for the pathway. As will be further discussed later, CPS is strongly allosterically inhibited by UMP, the eventual product of the pyrimidine biosynthetic pathway[20].

In prokaryotic systems activation of CPS as a function of ornithine is seen in the biosynthetic pathway for arginine (Figure 3). Arginine biosynthesis is carried out by the ligation of CP to ornithine to form citrulline. Citrulline is then converted via several enzymatic steps to form arginine. Ornithine activates CPS providing a feed forward mechanism for the production of arginine in non-ureotelic organisms. The urea cycle, while not present in prokaryotes, is critical for detoxification in organisms that use urea for nitrogen excretion. The urea cycle contains the same enzymes as the pathway for arginine biosynthesis with the addition of arginase, which liberates urea from arginine and closes the urea cycle with the reformation of ornithine. In Figure 3, it is again evident that CPS plays a key role in the metabolism of nitrogen, as carbamoyl phosphate reacts with ornithine to produce citrulline, which serves as an entry point to the urea cycle. Other than the reaction catalyzed by CPS, the reactions of the urea cycle are governed by substrate availability. CPS is potently allosterically activated by L-ornithine.

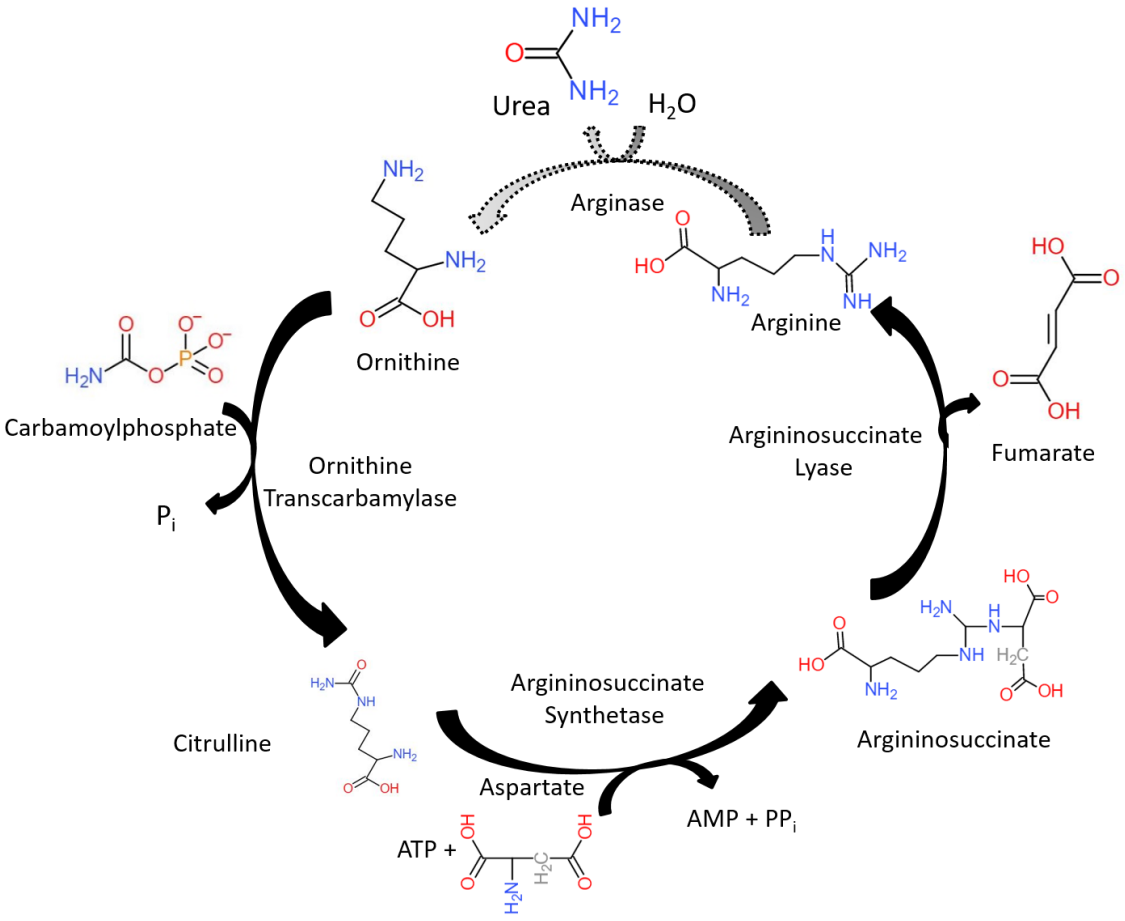

Figure 3: Representation of arginine biosynthesis (solid black arrows) and the urea cycle in ureotelic organisms (inclusion of arginase step in dotted arrow). Both demonstrate the feed forward mechanism of activation of CPS by ornithine.

From the examples provided, which is by no means an exhaustive list of allosteric enzymes, one can begin to appreciate the importance and wide ranging impact of this method of regulation. Recognizing that allosteric regulation is widespread in cellular processes leads one to consider the possibility of exploiting this phenomenon for pharmaceutical purposes. Allosteric regulation has potential as an emerging area of drug development, and it provides several advantages over more traditional competitive inhibitors or covalent inhibitors.

Naproxen is an extremely common generic drug used to treat inflammation, fever, and rheumatoid arthritis. It was first introduced in 1976 as Naprosyn; later, in 1994, naproxen was introduced as an over-the-counter medication under the brand name Aleve[21]. Naproxen acts as a competitive inhibitor of cyclooxegenase-1 and cyclooxygenase-2 (COX-1 and COX-2) in the biosynthesis of prostaglandins.

Prostaglandins have many functions in human physiology, which range from homeostatic regulation of tissues, inflammation and fever induction, and labor induction during pregnancy among others. The prostaglandin precursor, prostaglandin G_2, is synthesized from arachidonic acid by COX-1 and COX-2. COX-1 produces the prostaglandins that are responsible for homeostatic processes, and it is constitutively expressed, while COX-2 is inducible and responsible for inflammatory and fever response[22].

The binding pocket for arachidonic acid is similar in the two isoforms of COX-1 and COX-2; therefore, the competitive inhibitor binds both isoforms[23]. The binding of naproxen to both isoforms is why limits are placed on the use of naproxen. When taken for extended periods of time, the inhibition of COX-1 by naproxen results in stomach ulcers due to the lack of prostaglandin control of gastric acid secretion,[24] because naproxen does not discriminate between COX-1 and COX-2 . However, the competitive nature of naproxen inhibition enables quick recovery of homeostatic regulation when naproxen use is discontinued. Non-selectivity is not problematic to all competitive inhibitors, but the need for a high affinity, bioavailable substrate mimic is challenging.

To alleviate the impact of non-selective COX inhibitors, the drug Celebrex, valdecoxib, was developed in the 1990s and then approved by the Food and Drug Administration in 2001[23]. Still a competitive inhibitor, valdecoxib was the result of structure-aided drug design. When naproxen and other early non-steroidal anti-inflammatory drugs were developed, there were no molecular models of the target COX enzymes. The generation of molecular models, via x-ray crystallography, of COX-1 and COX-2 enabled scientists to make educated guesses about compounds that would selectively bind COX-2, based on detailed understanding of the differences between the binding pockets of the two isoforms[25]. This alleviated the adverse side effects of inhibition of COX-1; valdecoxib is a reversible, selective inhibitor of the COX-2 enzyme. Celebrex is currently prescribed for rheumatoid arthritis, osteoarthritis, and acute pain management.

Another strategy in drug development uses irreversible inhibitors. Irreversible inhibitors react with the enzyme and form covalent bonds, usually at the active site. These inhibitors permanently inactivate the enzyme by disrupting active site chemistry. This type of inhibition has a long history. Aspirin is an anti-inflammatory drug that targets the COX enzymes. However, instead of competing for the binding site in a reversible manner, aspirin acetylates the active site serine of both COX enzymes[26]. The acetylation of the active site prevents chemistry from occurring and blocks prostaglandin synthesis. Aspirin is also a non-selective inhibitor of COX family enzymes.

A common theme between competitive and irreversible inhibitors is that they mimic the substrate of the targeted enzyme. A problem arises when a targeted enzyme

shares a common substrate with other non-target enzymes; the COX enzyme family is only one example. Another way to treat disease states is with allosteric effectors which avoid the pitfalls of the drug types discussed thus far.

Developed in 2009 as a blood thinner, ticagrelor is an allosteric regulator of the platelet aggregation receptor $P2Y_{12}$[27]. $P2Y_{12}$ is a G-coupled protein receptor expressed on the extracellular surface of platelet cells. When ADP binds to the receptor, downstream signaling initiates platelet aggregation and subsequent clotting events[28].

Ticagrelor selectively inhibits $P2Y_{12}$, and it does not compete for the ADP binding site; therefore it is an allosteric inhibitor[29]. It is also a pharmacologically active compound that is immediately bioavailable upon infusion[28]. These two characteristics of ticagrelor address the issues with the previous generation of drugs. With a rapidly bioavailable compound, treatment is rapid, as opposed to 4–6 days for previously developed drugs[28]. Also, the termination of the effects is much more efficient due to the reversible nature of the inhibition.

Allosteric regulators as drugs have another advantage over traditional competitive and irreversible inhibitors. Allosteric regulators are not necessarily substrate analogs, which presents the opportunity to reduce non-specific interactions with enzymes or proteins that also use the substrate mimicked by the more traditional drugs.

As allosteric regulators are becoming the targets of drug design, it is important to understand the underlying principles of allosteric regulation. Extensive work on understanding allostery has been published, but there are still questions to answer with novel research.

Concepts of Allostery and a Model-Free Analysis

Understanding allosteric regulation requires a slight digression and the explanation of several concepts. As discussed earlier, allostery means that a ligand can induce a shift in conformational populations of proteins that results in saturable changes in the function of the allosteric protein.

According to the Monod, Wyman and Chengeaux (MWC) model for allostery, there are two possible states for an allosterically inhibited enzyme: the active form and the inhibitor-bound inactive form. The active form of the enzyme binds substrate and catalyzes the generation of products. The inhibitor-bound form, on the other hand, is traditionally considered inactive and essentially "turned off." From a simplistic viewpoint, this concept is sound; if the enzyme needs to be inhibited, it is "off." However, two states do not describe the whole story.

The two-state model can be interpreted as a single-substrate single-modifier system, depicted in Scheme 1. The enzyme, E, is capable of binding either substrate, A, or inhibitor, X, but it cannot bind both.

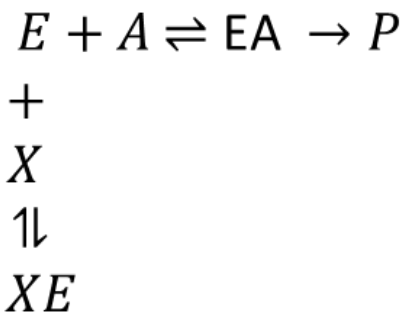

Scheme 1: Single-substrate competitive inhibitor scheme in which an inhibited enzyme (XE) is unable to bind substrate or undergo catalytic turnover.

This scheme presents a clear problem when one considers that enzymes are capable of catalytic turnover even when saturated with an allosteric inhibitor[30,31]. A fourth form of the enzyme in addition to the free enzyme and the binary complexes of enzyme and substrate, EA, and enzyme with inhibitor, XE, is missing. The fourth form must be a ternary complex of XEA, with enzyme bound to both substrate and inhibitor. McGresham's and Reinhart's work with *Thermus thermophilus* PFK is one example of an enzyme that exhibits tight binding of the allosteric effector, PEP, with weak inhibition. This enzyme in particular enables the investigation of the XEA complex because saturating levels of substrate and PEP can be simultaneously attained[32,33]. Unfortunately, the two-state model in Scheme 1 does not accommodate the ternary complex.

Depicted in Scheme 2 is a single-substrate single-modifier system that accounts for the formation of a ternary complex. This scheme accounts for the formation of the ternary complex, and it closes a thermodynamic box, which enables description of the binding of both ligands and dissociation constants for each binding event[34,35].

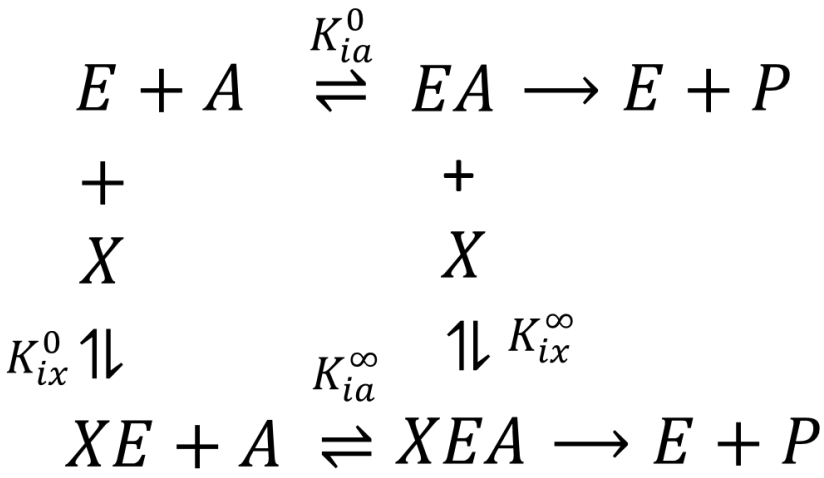

Scheme 2: Single-substrate, single-modifier scheme in which the inhibited enzyme can bind both allosteric effector (X) and substrate (A) to produce a catalytically active ternary complex (XEA). Thermodynamic dissociation constants can be determined for each binding event. $\boldsymbol{K_{ia}^{0}}$: E binding A. $\boldsymbol{K_{ia}^{\infty}}$: XE binding A. $\boldsymbol{K_{ix}^{0}}$: E binding X. $\boldsymbol{K_{ix}^{\infty}}$: EA binding X.

Using Scheme 2, one can define dissociation constants in terms of substrate, modifier, and enzyme. Reinhart demonstrated that the quantity Q_{ax} is a measure of the nature and magnitude of an allosteric effector on the binding of substrate[35]. He defined Q_{ax} as the ratio of K_{ia}^{0} to K_{ia}^{∞}, and when an allosteric effector causes the dissociation constant of A to increase, Q_{ax} will become less than unity. By contrast, if the effector causes the dissociation constant of substrate to decrease, Q_{ax} will become greater than unity. Reinhart's theory enables model-free quantification of the allosteric effect while indicating whether the effector is inhibitory or activating. Furthermore, since the dissociation constants can be manipulated to generate the disproportionation equilibrium, as follows in Reaction 1, Q_{ax} is the equilibrium constant for the disproportionation equilibrium.

(1) $$EA + XE \rightleftharpoons E + XEA$$

Since Q_{ax} is an equilibrium constant, the allosteric effect can be quantified as ΔG_{ax}, which is the coupling free energy between the substrate and the allosteric ligand. Discussing allostery from a thermodynamic standpoint enables investigations of the fundamental contributions of enthalpy and entropy to the allosteric interaction in a model-free manner.

Several enzymes have been studied in this manner by the Reinhart group, including many prokaryotic PFK enzymes, human and murine PFK isoforms, glycogen phosphorylase from rabbit muscle, isocitrate dehydrogenase, and prokaryotic CPS[8,20,32,36–40]. This work uses the model enzyme CPS from *Escherichia coli.* However, the complicated stoichiometry, complex coordination of multiple reaction centers, use of a molecular tunnel of approximately 96 Å in length, and the critical allosteric regulation of CPS requires a bit of introduction to the enzyme of interest.

Carbamoyl Phosphate Synthetase

CPS from *E. coli* is an αβ heterodimer. The two subunits catalyze specific parts of the overall synthesis of carbamoyl phosphate, resulting in the conversion of glutamine, bicarbonate, and two equivalents of MgATP to glutamate, two equivalents of MgADP, and carbamoyl phosphate (Reaction 2). The smaller of the two subunits is responsible for generation of the nitrogen found in the end product. The small subunit

catalyzes the deamidation of glutamine to glutamate and the diffusible intermediate ammonia.

Sequestering the diffusible intermediate is critical for the enzymatic activity because the next reaction center is in the second of the two subunits. CPS sequesters ammonia, and other diffusible intermediates, using an intramolecular tunnel similar to that found in tryptophan synthetase however, the tunnel found in CPS is much longer[41]. With regard to the sequestering of ammonia, the molecular tunnel runs from the glutaminase reaction center across the dimeric interface to the carboxyphosphate synthesis reaction center. The second reaction center is where bicarbonate and one equivalent of MgATP are used to synthesize carboxyphosphate (Reaction 3). Also, at this reaction center, ammonia is delivered and reacts with the high energy carboxyphosphate, resulting in the formation of carbamate and inorganic phosphate. The product of the second reaction, carbamate, is very reactive and quickly degrades when exposed to bulk solvent.

Through the continuation of the tunnel, bulk solvent is prevented from interacting with the substrate while it is shunted to the third, and final, reaction center. The carbamoyl phosphate synthetic center consumes another equivalent of MgATP and the carbamate delivered via the tunnel to produce the final product of carbamoyl phosphate and MgADP (Reaction 4). These reactions all produce reactive and/or diffusible species and must be timed correctly to prevent the buildup of intermediates.

(2) $$L-Glutamine\ +2MgATP\ +HCO_3^-\rightarrow Carbamoyl\ phosphate+\ L-Glutamate+\ 2MgADP$$

(3) $HCO_3^- + MgATP + NH_3^+ \rightarrow MgADP + Carbamate$

(4) $Carbamate + MgATP \rightarrow Carbamoyl\ Phosphate + MgADP$

The final product of the reactions catalyzed by CPS is at the nexus of two critical biochemical pathways. Carbamoyl phosphate (CP) can combine with L-ornithine to produce citrulline and enters the urea cycle in ureotelic organisms. In prokaryotes the citrulline is used for arginine biosynthesis (Figure 3). Carbamoyl phosphate can also ligated to aspartate by aspartate transcarbamylase and proceed through pyrimidine biosynthesis to form UMP and CTP (Figure 2). Carbamoyl phosphate is an important metabolite in cellular processes and as such there is significant regulation of the catalytic activity of CPS. This is indeed, the case. CPS is allosterically regulated by downstream products of the biosynthetic pathways, into which carbamoyl phosphate feeds. L-ornithine, an allosteric activator, is the final (and first) substrate in the urea cycle. As such, buildup of L-ornithine indicates an imbalance and the need for higher carbamoyl phosphate production. L-ornithine activates CPS by increasing the binding affinity of MgATP by over 15-fold[20,31]. Alternatively, a surplus of the pyrimidine nucleotide UMP indicates increased flux through the pyrimidine biosynthetic pathway, and CP production should be attenuated. UMP binds CPS at a site unique from L-ornithine and allosterically inhibits the production of CP by significantly reducing the affinity for MgATP [20,31,39].

The heterodimeric, multidomain structure of CPS makes it interesting for detailed biochemical and biophysical studies of enzymatic allostery. The heterodimeric enzyme has a molecular weight of 160 kDa; the constituent subunits weigh 118 kDa (large subunit) and 42 kDa (small subunit). The work of Anderson, Meister and, others in the 1960's and 70's provided the first biochemical characterization of CPS[42–44]. Their work was later fleshed out and confirmed by Raushel, Villafranca, Holden, Reinhart, Braxton and others. There are three reaction centers located on CPS that are separated in space by approximately 100 Å (as the substrate travels)[45]. Glutaminase activity occurs in the small subunit; it has a protein fold similar to that found in GMP synthetase and exhibits hallmarks of the α/β-hydrolase fold family of proteins[46]. The carbamate synthesis catalytic site is located 45 Å from the glutaminase activity, and occurs in the second subunit of CPS. The synthetase subunit, or large subunit, is considered to have been generated as a result of gene duplication[47]. This assertion is supported by the x-ray crystallographic model proposed by Thoden et al. in which the two synthetic domains of the large subunit are related by a 2-fold rotational axis[48]. The final reaction center of CPS is also a synthetase reaction. The carbamoyl phosphate synthetase center is located 25 Å away from the carbamate synthesis reaction, and the allosteric domain of CPS is directly adjacent to this domain. Figure 4 is the x-ray crystallography structure reported by Thoden et al. and provides a visual representation of the spatial orientation of the reaction centers and allosteric domains[48].

Figure 4: X-ray crystallography structure of CPS from *E. coli.* The domains are color coded as follows: small subunit, blue; carboxyphosphate domain, green; carbamoyl phosphate domain, teal; oligomerization domain, purple; and allosteric domain, red. Based on PDB file 1JDB[49].

The allosteric domain harbors two distinct binding sites: one for L-ornithine, an activator, and one for the pyrimidine nucleotides UMP and IMP[50,51]. The binding pockets and allosteric effects have been previously characterized[50,52–54].

Braxton et al. extensively characterized the allosteric response of CPS as a heterodimer[20,31,55,56], which serves as the basis for the research presented herein. As such, a dedicated description of that work will be undertaken.

First, the effects of ornithine, UMP, and IMP were determined for each reaction center of CPS. Due to the complex stoichiometry of the full forward reaction of CPS (see Reaction 2), the effect of the allosteric ligands cannot be separated into individual

binding events or the catalytic turnovers of particular reactions. However, the forward reaction demonstrates a robust response to both the activator ornithine and the inhibitor UMP[20].

Investigation of the partial reactions independently enabled a more detailed understanding of how allosteric effectors impact the binding and turnover of ligands. The bicarbonate dependent ATPase reaction (Reaction 3) is moderately impacted upon allosteric ligand binding. Ornithine causes a 2-fold decrease in the dissociation constant for MgATP and a 1.5 fold decrease in the Michaelis constant for bicarbonate, while the V_{max} is not appreciably affected[20].

ATP synthesis by CPS (Reaction 4), the reverse of the carbamoyl phosphate synthesis reaction, was also investigated and demonstrated some remarkable characteristics. The ordered nature and complex stoichiometry of the forward reaction of CPS raised questions about the kinetic mechanism of the ATP synthesis reaction. Braxton et al. demonstrated that the kinetic mechanism of the ATP synthesis reaction appeared to be rapid equilibrium ordered[20]. The impact of the allosteric ligands, ornithine and UMP, on the ATP synthesis reaction were also reported. Ornithine has a very profound impact on the thermodynamic dissociation constant, which is distinct from the Michaelis constant, for MgADP, lowering it by 18-fold. UMP also has a dramatic effect on the binding of MgADP, causing a 15-fold increase in K_{ia}. Ornithine and UMP, however, do not affect the binding of CP to the enzyme, and the K_b remains 1.6 mM. Interestingly, ornithine and UMP have different effects on the V_{max} of the ATP

synthesis reaction. Ornithine has no effect on the maximal velocity, while UMP causes a 68% decrease[20].

Foundation for Work Presented

In a report published in 1996, Braxton et al. investigated the thermodynamics of allosteric regulation in CPS. They demonstrated that the effect of both ornithine and UMP exhibited an entropy-dominated characteristic in the coupling free energy[56]. Braxton et al. made extensive use of the methodologies published by Reinhart et al. in 1989, demonstrating that the allosteric coupling parameter Q_{ax} could be monitored at various temperatures, and through Van't Hoff analyses, the entropic and enthalpic components of the allosteric effect could be determined[57].

Here, I seek to further take advantage of the methodology presented in 1989 by Reinhart et al.[57] and investigate perturbations to the entropic component of the allosteric effect in CPS by removing the glutaminase subunit.

The large subunit of CPS retains the ability to catalyze the partial reactions of bicarbonate dependent ATP hydrolysis, ATP synthesis, and complete carbamoyl phosphate synthesis, when provided with ammonia[58]. In light of the entropy-dominated nature of the allosteric effects of ornithine and UMP in the heterodimer, I hypothesize that the large subunit, when expressed and purified in isolation from the small subunit, and investigated using steady-state kinetics will demonstrate an enhanced entropic component of the allosteric coupling free energy of ornithine and UMP and augment their respective effects. Here, I present evidence that liberation of the subunit interface

has profound impacts on the kinetic mechanism (Chapter III) of the ATP synthesis reaction, the allosteric effect of UMP on both partial reactions (Chapter IV), and the allosteric effect of ornithine on the partial reactions (Chapter V) of the large subunit of CPS from *E. coli*.

CHAPTER II

GENERAL MATERIALS AND METHODS

All chemicals used in the preparation of buffers for purification, dialysis, electrophoresis or, enzymatic assays were of analytical grade and purchased from either Sigma Aldrich (St. Louis, MO) or Fisher Scientific (Fair Lawn, NJ). Enzymes used in the coupled assay systems were purchased from Roche (Indianapolis, IN) as ammonium sulfate suspensions. ATP, ADP, $KHCO_3$, and carbamoyl phosphate (CP) were purchased from Sigma Aldrich. Resins used in chromatography were purchased from GE Life Sciences (Charlottesville, VA). $NADP^+$, NADH, DTT were purchased from Research Products International (Mt. Prospect, IL). Before use in enzymatic assays enzymes in ammonium sulfate solution were dialyzed against 50 mM HEPES, 0.5 mM EDTA at pH 7.5. Purification of plasmids was performed using the Qiagen plasmid mini-prep kit (Hilden,Germany).Only distilled deionized water was used in the preparation of buffers and chemical solutions.

Protein Purification

The isolation of heterodimeric and the large subunit of CPS were performed as described previously by Mareya and Raushel[59] with some modifications. Purification buffers used in isolating the heterodimer contained 10 mM L-ornithine, unless otherwise noted. Heterodimeric CPS was isolated from XL1-Blue cells containing the plasmid pMSO3 while RC-50 cells containing the plasmid pHN12 were used for the isolation of the large subunit of CPS[52,60,61]. Cells containing the appropriate vector were streaked for

isolation from a previously frozen glycerol stock on to Luria-Bertani agar plates containing 100 mg/mL ampicillin. After incubation for 16-18 hours at 37°C single colonies were picked from the agar plate and transferred to a 5mL Luria-Bertani liquid media also containing 100 mg/mL ampicillin. The liquid culture was incubated in a rotating drum for16-18 hours at 37°C allowing the culture to reach stationary phase. Several large scale (1.5L) Luria-Bertani medium with 100 mg/ml ampicillin were prepared and 500 µL of the 5mL culture was used to inoculate the prepared media. Again, the cultures were allowed to grow at 37°C to stationary phase (approx. 18 hours). Cell cultures were then pelleted via centrifugation in a Beckman J-6B for 25 min at 3,500xg at 4°C. Cell pellets were then stored at -80°C until purification of protein. Prior to protein purification the cell pellet was allowed to thaw at room temperature. After thawing, the cell pellet was suspended in 100 mM potassium phosphate, 0.5 mM EDTA, 10 mM L-ornithine at pH 7.5 and brought to a final volume of 80-100 ml. The cells were lysed using a Sonic Dismembrator model 550 sonication device (Fisher Scientific) for a total of 12 minutes (30 seconds on, 45 seconds off). The cellular lysate was clarified via centrifugation in a Beckman J-6B at 11,000xg for 25 minutes at 4°C. The clarified lysate was then treated with ammonium sulfate at 50% (w/w) and subjected to 6,500xg for 25 minutes at 4°C to pellet the precipitated proteins. The supernatant was concentrated with 65% ammonium sulfate in preparation for load on to a S-300 gel filtration column. The S-300 (25cm x 2.7cm) was equilibrated with 100 mM potassium phosphate, 0.5 mM EDTA, and 10 mM L-ornithine at pH 7.5. The concentrated protein pellet was resuspended in minimal volume (approximately 3 to 5mL) with buffer described above.

The suspension was then loaded to the S-300 column and run at 0.5mL/min collecting 4 mL fractions. Fractions were evaluated for the presence of CPS by 10% SDS-PAGE and enzymatic activity assays. Fractions containing CPS were pooled and dialyzed extensively against 50 mM Tris-HCl, 0.5 mM EDTA pH 7.5 to remove L-ornithine.

If significant contaminating proteins were visualized in an SDS-PAGE gel of pooled CPs fractions, an additional polishing step was performed using a High-Q resin from GE Life Science. The High-Q resin was equilibrated with the phosphate buffer above, without L-ornithine. Protein solution from dialysis was loaded on to the column and eluted with a 0-1 molar KCl gradient. Fractions were evaluated by SDS-PAGE and enzymatic activity assay. Fractions containing CPS activity were pooled and dialyzed against the TRIS-HCL buffer above. CPS solution was assayed via Pierce BCA assay kit from Thermo (Rockford, IL) for total protein concentration then aliquoted and stored at -80°C until use.

Enzymatic Assays

Bicarbonate Dependent ATPase

The consumption of MgATP to produce carbamate was monitored by coupling the production of MgADP to the oxidation of NADH through pyruvate kinase and lactate dehydrogenase as represented in Figure 5. Assays were initiated by addition of CPS or large subunit of CPS after temperature equilibration. A final volume of 0.6 mL contained 50 mM HEPES-KOH, 100 mM KCl, 20 mM $MgCl_2$ at pH7.5. Solutions of

substrates and allosteric effectors: $KHCO_3$, MgATP, L-ornithine, or UMP, were pH adjusted to 7.5. Concentrations of substrate and effector added were varied as described in the text. Spectral absorbance of the reaction mixture was followed at 340nm on a Beckman series 600 spectrophotometer.

ATP Synthesis

Synthesis of MgATP by both constructs of CPS was monitored through the coupling of MgATP to the reduction of $NADP^+$. The coupling was accomplished using hexokinase and glucose-6-phosphate dehydrogenase as the coupling enzymes as represented in Figure 6. Assays were initiated by addition of CPS or large subunit of CPS after temperature equilibration. A final volume of 0.6 mL contained 50 mM HEPES-KOH, 100 mM KCl, 20 mM $MgCl_2$ at pH 7.5. Solutions of substrates and allosteric effectors: MgADP, L-ornithine, UMP were pH adjusted to 7.5. Concentrations of substrate and effector added were varied as described in the text. In the case of the heterodimeric CPS, the mechanism for the synthesis of MgATP is equilibrium ordered[20]. This requires the concentration of the CP, second substrate, to be limited to sub-Km levels so that the kinetic dissociation constant approximates the thermodynamic dissociation constant. Spectral absorbance of the reaction mixture was followed at 340nm on a Beckman series 600. CP is an unstable compound, to ensure the accuracy of concentration and viability of the substrate a fresh solution of CP was made every hour from a previously aliquoted amount of CP stored at -20°C. Solutions of CP were kept on ice until added to cuvettes for kinetic assays.

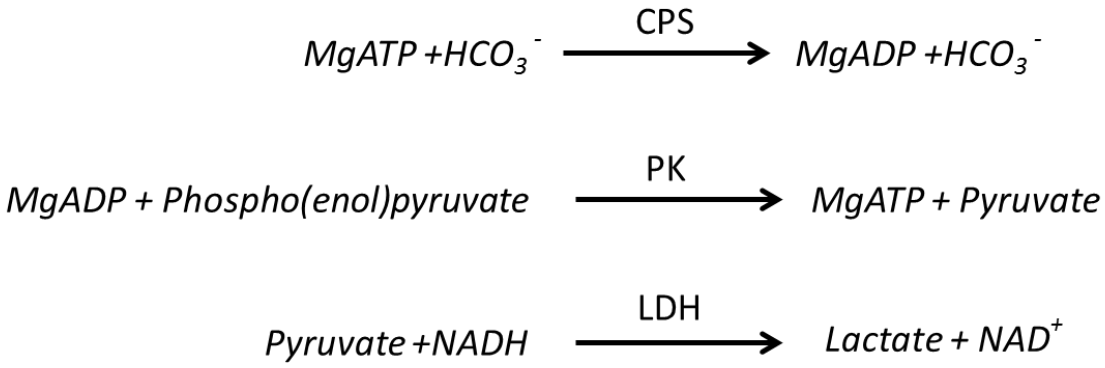

Figure 5: Coupled assay system used to monitor the consumption of MgATP. CPS generates MgADP, pyruvate kinase (PK) converts MgADP back to MgATP resulting in the production of pyruvate. Pyruvate is then reduced by lactate dehydrogenase as the cofactor NADH is oxidized to NAD^+. NADH absorbs light at 340nm while NAD^+ does not; thus allowing the tracking of MgATP consumption.

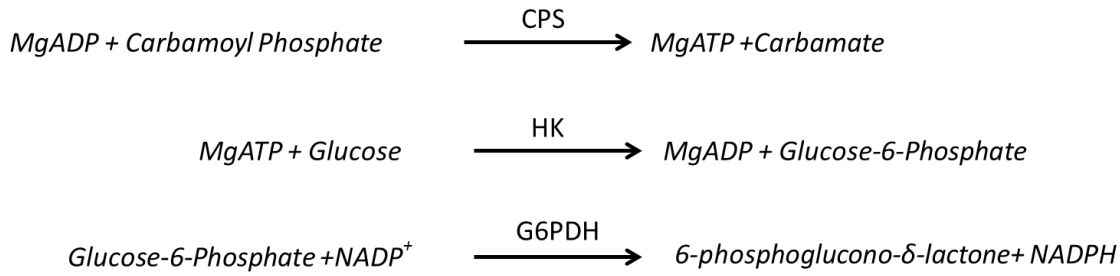

Figure 6: Coupled assay system used to monitor synthesis of MgATP. CPS generates MgATP from MgADP and carbamoyl phosphate. The formation of Glucose-6-phosphate is then catalyzed by hexokinase at the expense of the MgATP produced by CPS. The glucose-6-phosphate is then oxidized by glucose-6-phosphate dehydrogenase as $NADP^+$ is reduced to form 6-phosphoglucono-δ-lactone and NADPH. NADPH absorbs light at 340nm while $NADP^+$ does not; thus allowing the tracking of MgADP consumption.

CHAPTER III

LIBERATION OF THE SUBUNIT INTERFACE RESULTS IN AN ENHANCEMENT OF SEQUENTIAL MECHANISM CHARACTERISTICS

Introduction

Carbamoyl phosphate synthetase (CPS) from *E. coli* is an αβ heterodimer genetically encoded by the *carAB* gene pairs[60]. Translation of *carA* and *carB* result in polypeptides of 42 kDa and 118 kDa, respectively[62]. The heterodimer catalyzes the formation of carbamoyl phosphate at the expense of glutamine, bicarbonate, and two equivalents of MgATP as depicted in Figure 7[63].

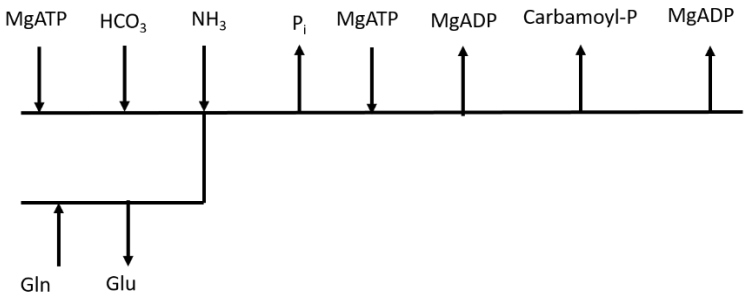

Figure 7: Kinetic reaction scheme for the synthesis of carbamoyl phosphate by CPS as reported by Raushel et al. in 1978[63]. This scheme represents the reaction when glutamine is used as a nitrogen source.

Coordinating the binding, catalysis of multiple reactions, intermediate sequestration, and product release of the complex reaction scheme shown above necessitates a multidomain enzyme. Each of the five domains of CPS has a distinct yet intertwined roll in the synthesis of carbamoyl phosphate.

The 42-kDa subunit is responsible for the formation of ammonia through the deamidation of glutamine to glutamate[64]. The other four domains all reside on the larger, 118kDa, subunit (Figure 8A). The carbamate synthesis domain activates bicarbonate at the expense of MgATP. The higher energy and more reactive, transient intermediate, carboxyphosphate is amidated to produce carbamate. The final reaction domain on CPS is the carbamoyl phosphate synthesis domain. The formation of the final product, carbamoyl phosphate, is accomplished through the phosphoryl transfer from the second equivalent of MgATP to carbamate. There are also two important non-cactalytic domains in CPS. The oligomerization domain regulates the association of the αβ heterodimer into it higher order structures. Kim and Raushel demonstrated the order in which the complete $(\alpha\beta)_4$ oligomer assembled[65]. They reported that an elongated dimer forms first by association through the allosteric domain followed by the association of two elongated dimers through the oligomerization domain. The oligomerization is mediated by effectors of CPS, ornithine and inosine monophosphate, which bind to the fifth domain, the allosteric domain. The allosteric domain of CPS binds three allosteric effectors; ornithine, UMP, and IMP[49,66,67]. Ornithine activates CPS by increasing the affinity for substrates[20,31]. UMP inhibits the binding of substrates[20,39]. IMP is a weak inhibitor at physiological temperatures but, shows an activation effect at higher temperatures[20,55]. As previously stated, ornithine and IMP not only affect substrate affinity but also mediate the formation of higher order oligomers of CPS.

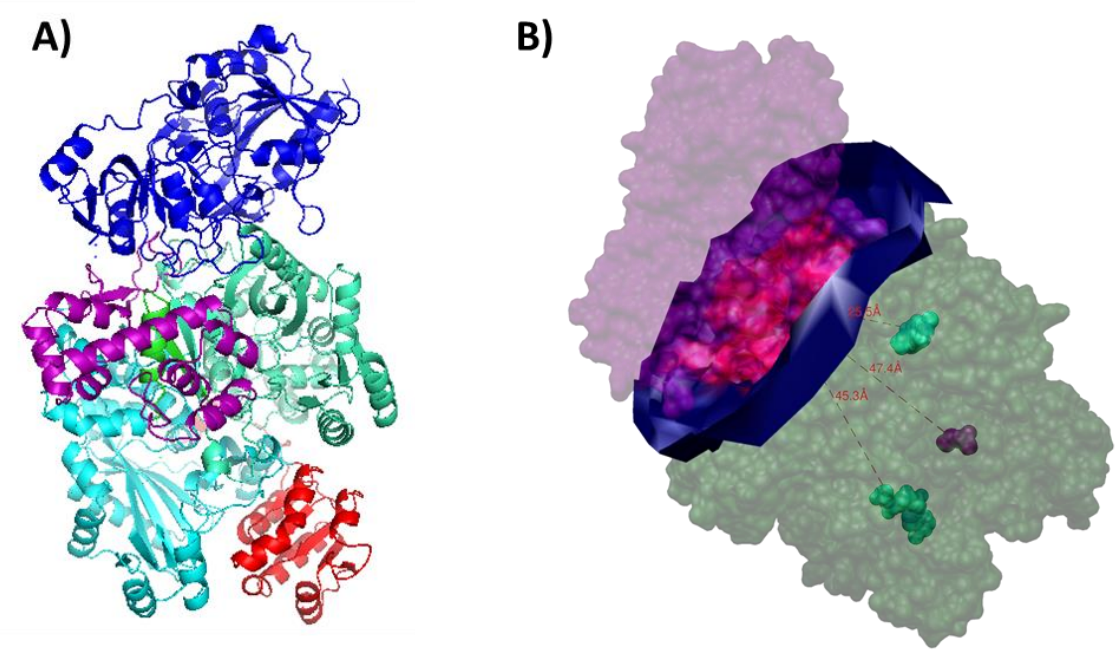

Figure 8: A) Domains of CPS colored: Blue- Glutaminase domain, Blue-green- Carboxy phosphate domain, Cyan- Carbamoyl phosphate domain, Red- Allosteric Domain, Purple- Oligomerization domain. Based on PDB ID: 1JDB. B) Space fill model of 1JDB highlighting the interface of the αβ dimer and the distances of MgADP(green) and L-Ornithine (purple) from the dimeric interface. The teal MgADP space filled atoms represent the locations of the ATPase and the ATP synthesis reaction centers. The blue collar around the interface is an artifact of the interface surface script in Chimera(UCSF).

Despite the complexity of heterodimeric CPS the partial reactions of each catalytic center have been well studied[58,44,68]. The forward reaction (1), bicarbonate dependent ATPase partial reaction (2), carbamoyl phosphate synthesis reaction (3), and ATP synthesis reaction (4) have been characterized with respect to affinities and structures of the binding pockets[20,58,66,69–71]. As is evident in Figure 8B, the reaction centers of CPS are located in spatially distinct regions of the polypeptide. The spatial separation of the reaction centers produces a unique problem upon consideration of the reactive nature of the some intermediates and the possibility of intermediates diffusing away from the enzyme[72]. CPS contains an intramolecular tunnel that sequesters intermediates from bulk solvent, and provides a mechanism for the coordination of reaction centers such that intermediates are not wasted[73,74].

(1) $$Gln + HCO_3^- + 2MgATP \rightarrow Glu + 2MgADP + CP + P_i$$

(2) $$HCO_3^- + MgATP \rightleftharpoons HCO_3^- + MgADP + P_i$$

(3) $$Carbamate + MgATP \rightleftharpoons CP + MgADP$$

(4) $$CP + MgADP \rightleftharpoons Carbamate + MgATP$$

(5) $$NH_3 + HCO_3^- + 2MgATP \rightarrow 2MgADP + CP + P_i$$

Of particular interest is the ATP synthesis reaction of CPS. The synthesis of ATP is catalyzed by the carbamoyl phosphate reaction center operating in the reverse direction[44]. Reaction 4 has been shown to exhibit the strongest response to allosteric regulators and operate with K_d values within an achievable range for all ligands in vitro[39]. Also of note, is the spatial proximity of the ATP synthesis reaction to several key

elements of the CPS enzyme. As depicted in Figure 8A the allosteric domain is proximal to the catalytic site for ATP synthesis. The activator, L-ornithine, binds less than 15 Å from MgADP in the active site and electron density in crystal structures indicates that it bridges the allosteric domain and the carbamoyl phosphate synthesis domain. Synthesis of ATP is also carried out at the reaction site most distal from the heterodimeric interface, approximately 45 Å[49].

Due to the fact that the large subunit contains all domains except for the glutaminase domain, the large subunit can catalyze reactions 2-4 when purified in isolation from the smaller subunit. Both the large subunit of CPS in isolation, as well as the heterodimer, are also capable of catalyzing the synthesis of CP when ammonia is provided according to reaction (5)[58]. However, there are impacts on the turnover and binding constants for each of the catalytic centers when interrogated in the absence of the small subunit[43,58].

In studies of the allosteric response of heterodimeric CPS, Braxton et al. reported in 1992 that the ATP synthesis reaction proceeds through an equilibrium ordered kinetic mechanism[20]. The kinetic mechanism of the ATP synthesis reaction was unclear due to the ordered nature of the forward reaction proposed by Raushel et al. in 1978[63]. Determination of the kinetic mechanism permitted the use of steady-state kinetics, with some accommodation, to determine an approximation of the thermodynamic dissociation constants for MgADP and the allosteric regulators as described by Reinhart[34]. One important accommodation in the steady-state experiments performed by Braxton was to limit the concentration of the CP to sub-K_m concentrations in order for the K_m to

approximate the K_d and assure that the dissociation constant observed was that of MgADP.

As the overall goal of my research is to investigate the thermodynamics of allosteric regulation in CPS, as a heterodimer and within the large subunit in isolation, it is necessary to determine if ATP synthesis proceeds through an equilibrium ordered mechanism when the small subunit is removed. Here I present data supporting the argument that the synthesis of ATP by the carbamoyl phosphate reaction center of CPS proceeds through a sequential mechanism when the large subunit is interrogated in isolation.

Methods

Wild type, heterodimer and large subunit, CPS was grown in 1.5 L LB/Ampicillin (100 mg/ml) at 37°C for 18 hours. The cells were harvested via centrifugation in a Beckman D4 centrifuge. Cellular pellets were stored at -20°C until purification of protein. Protein purification proceeded as described in the previous chapter. Initial velocity kinetic experiments were conducted using both enzyme constructs. The rate of ATP synthesis was monitored using a coupled assay system consisting of hexokinase and glucose-6-phosphate dehydrogenase (RPI) that couples the production of ATP by CPS to the conversion of $NADP^+$ to NADPH (Roche). The production of NADPH can be monitored using UV/Vis spectrophotometry at 340 nm using a Beckman DU-40 spectrophotometer. Kinetic experiments were conducted in 600

µl final volume containing: kinetics buffer (50 mM NaHEPES, 10 mM KCl, 20 mM $MgCl_2$, 0.5 mM EDTA, pH 7.5), coupling enzymes (4U Hexokinase, 4U G6PDH), 10 mM glucose, 2 mM $NADP^+$, and varying concentrations of MgADP and CP (Sigma). CP solutions were made fresh, hourly, from pre-weighed lithium carbamoyl phosphate stored at -20°C. The enzymatic rates of CPS were restricted by dilution of enzyme such that no more than 10% of available substrate was consumed while monitoring the reaction. Initial plots were constructed using Kaleidagraph data analysis software (Synergy Inc.) and multivariate fitting was performed with IgorPro multivariate fitting analysis (WaveMetrics). Data were fit to the following initial velocity rate equations as appropriate.

(1) $$\frac{v_0}{E_T} = \frac{V_{max}[A]}{K_a + [A]}$$

(2) $$\frac{v_0}{E_T} = \frac{V_{max}[A][B]}{K_{ia}K_b + K_b[A] + [A][B]}$$

(3) $$\frac{v_0}{E_T} = \frac{V_{max}[A][B]}{K_{ia}K_b + K_b[A] + K_a[B] + [A][B]}$$

Equation (1) is used to fit data following Michaelis–Menten kinetics and allows determination of the Michaelis constant for the varied substrate, K_a, and the maximal velocity of the reaction under the experimental conditions, V_{max}. Equation (2) describes an equilibrium ordered kinetic mechanism in which K_{ia} is the thermodynamic dissociation constant for the first substrate (in these experiments, MgADP) and $K_b$is the

Michaelis constant for the second substrate, CP. Equation (3) describes a sequential mechanism with the terms being the same as described above.

Results

Heterodimer

Heterodimeric CPS was isolated as described in Chapter II. Initial velocities were determined at various concentrations of both MgADP and carbamoyl phosphate. When data from these experiments are plotted with the reciprocal of the initial velocities as a function of reciprocal concentration of the varied substrate; the double reciprocal plot displays an intersecting pattern that is indicative of an sequential mechanism [75,76](Figure 9). Secondary plots of the slope and intercept as a function of second substrate concentration have the potential to give more detailed insight into the kinetic mechanism of the ATP synthesis reaction. Neither replot of the slope and intercept as a function of 1/[MgADP] nor 1/[CP] reveal much since there are no defining features present to indicate a more specific mechanism than that of sequential addition (Figure 10). For example, the replot of slope values from Figure 9 do not extrapolate to the origin, which would indicate an obligatory order of addition for the substrates and suggest an equilibrium ordered kinetic mechanism. These data are not in agreement with literature[20]. However, the discrepancy between K_a for MgADP of 16 μM, derived from the fit to Equation 3, and the lack of K_a in previous work may result from experimental differences; including instrumentation sensitivity, substrate ranges and/or, reagent purity. The patterns of the primary plots when evaluated in conjunction with trends in the

secondary plots provide evidence that the ATP synthesis reaction proceeds with sequential addition of substrates. The data were fit to rate equations 2 and 3 described above and the resulting parameters derived there from are identified in Table 1.

The fit lines of the data presented in Figure 9 and Figure 11 are representative of the global fit of the respective data sets. IgorPro was used to fit the data to equation 3 resulting in values displayed in Table 1. These values were used to generate lines representing the double reciprocal plots expected from those values and the experimental concentrations of carbamoyl phosphate and MgADP.

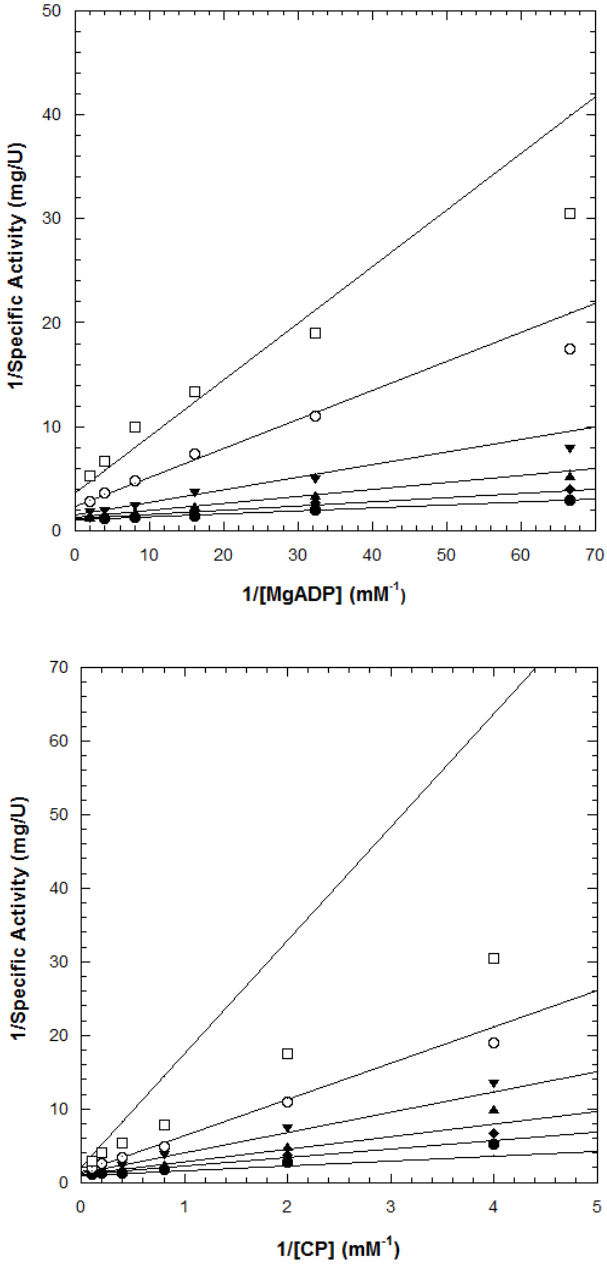

Figure 9: Double reciprocal plots for the initial velocity data of heterodimeric CPS. Top) Specific activity of ATP synthesis as a function of MgADP at fixed concentrations of carbamoyl phosphate, closed circles 10 mM, closed diamonds 5 mM, closed triangles 2.5 mM, closed inverted triangles 1.25 mM, open circles 0.5 mM, open squares 0.25 mM. Bottom) Specific activity of heterodimeric CPS ATP synthesis as a function of carbamoyl phosphate at fixed concentrations of MgADP, closed circles 0.5 mM,closed diamonds 0.25 mM, closed triangles 0.125 mM, closed inverted triangles 0.062 mM, open circles 0.031 mM, open squares 0.015 mM.

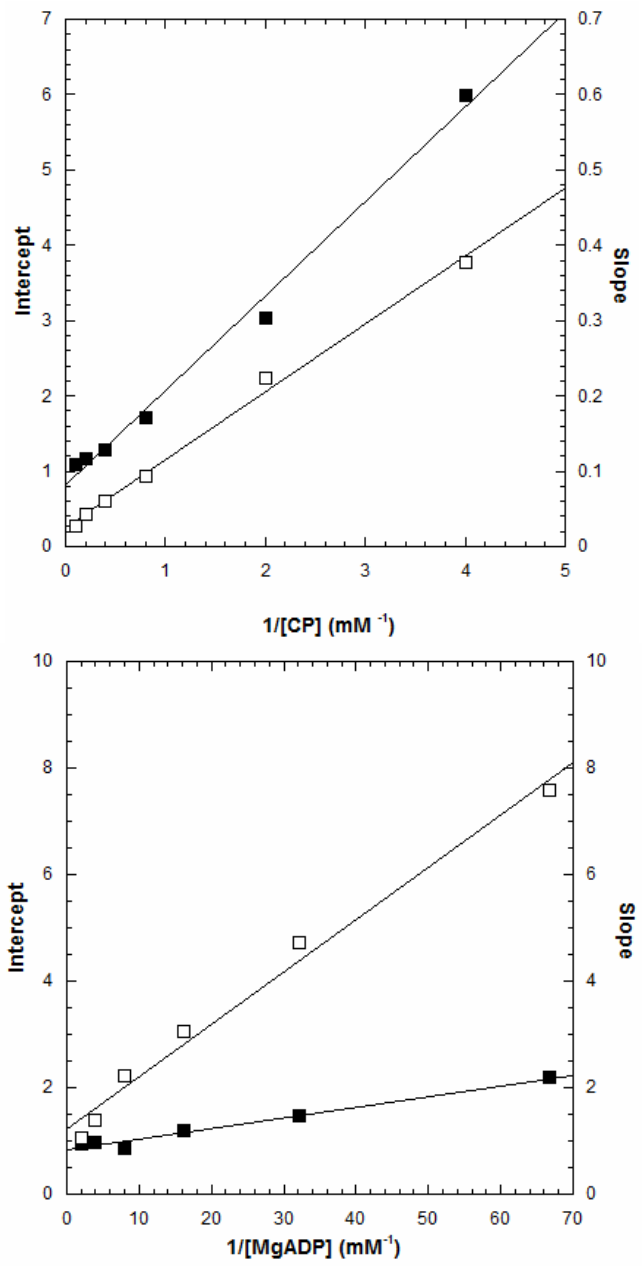

Figure 10: Secondary plots of Slope and Intercept values for heterodimeric CPS experiments: Top) Secondary plot of the Slope and intercept values from the primary plot in which MgADP was varied at fixed concentrations of CP. closed squares- Intercept, open squares-Slope. Bottom) Secondary plot of the Slope and intercept values from the primary plot in which CP was varied at fixed concentrations of MgADP. Closed squares- intercept, open squares- slope.

Large Subunit

Isolated large subunit was subject to the same experimentation performed with the heterodimer. The primary plot of ATP synthesis activity as a function MgADP at fixed concentrations of CP demonstrates an intersecting pattern (Figure 11) and is generally unremarkable. The plot of ATP synthesis activity as a function of CP at fixed concentration of MgADP however, varies from the behavior observed in the experiments with heterodimer (Figure 9). Comparing behavior seen in Figure 11 with Figure 9 it is evident that the intersection of the fit lines for the data at fixed MgADP concentration is significantly displaced from the y-axis however, examination of the secondary plots of slope and intercept (Figure 12) provide further evidence of the deviation of the kinetic constants in the large subunit from that of the heterodimer. When CP is held constant in kinetic experiments and the secondary plots of slope and intercept are generated (Figure 12), it is evident that the fit line of the slope parameter extrapolates to the x-axis at a point significantly displaced from the origin compared to the data with the heterodimer. The secondary plot for the experiments with CP held constant is, as with the heterodimer, is only diagnostic of a sequential mechanism.

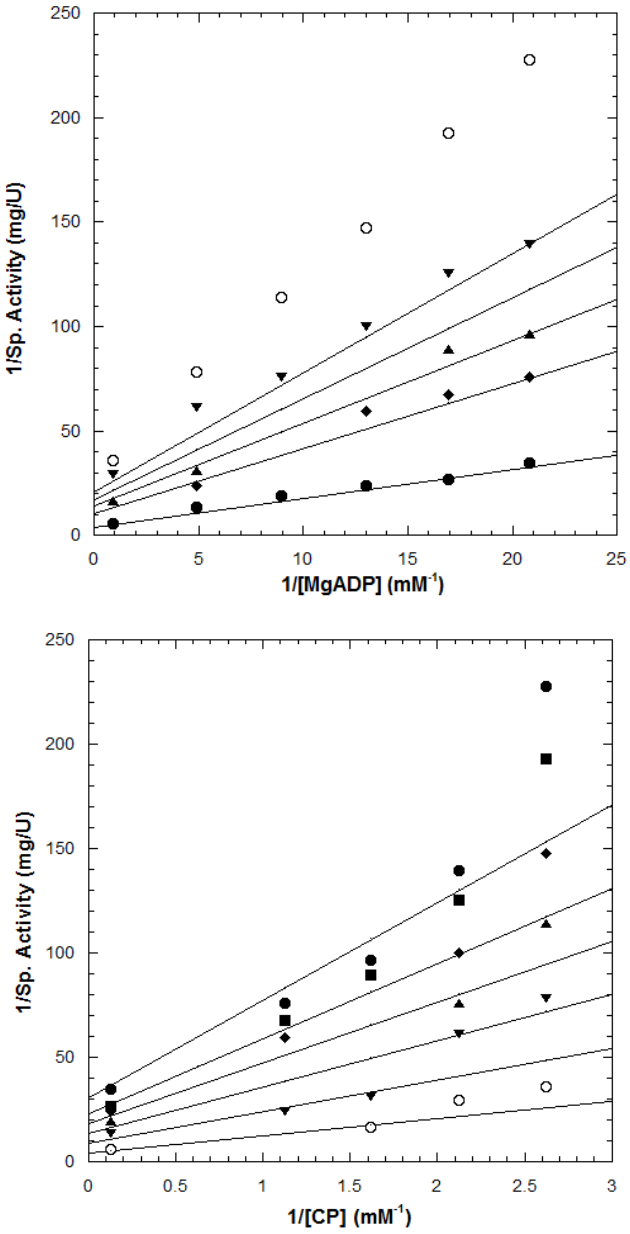

Figure 11: Double reciprocal plots for the initial velocity data of the large subunit. Top) Specific activity of CPS ATP synthesis as a function of MgADP at fixed concentrations of carbamoyl phosphate, closed circles 8 mM, closed diamonds 0.89 mM, closed triangles 0.62 mM, closed inverted triangles 0.47 mM, open circles 0.38 mM. Bottom) Specific activity of CPS ATP synthesis as a function of carbamoyl phosphate at fixed concentrations of MgADP, closed circles 0.048 mM, closed squares 0.059 mM, closed diamonds 0.077 mM, closed triangles 0.112 mM, inverted triangles 0.204 mM and, open circles 1.1 mM.

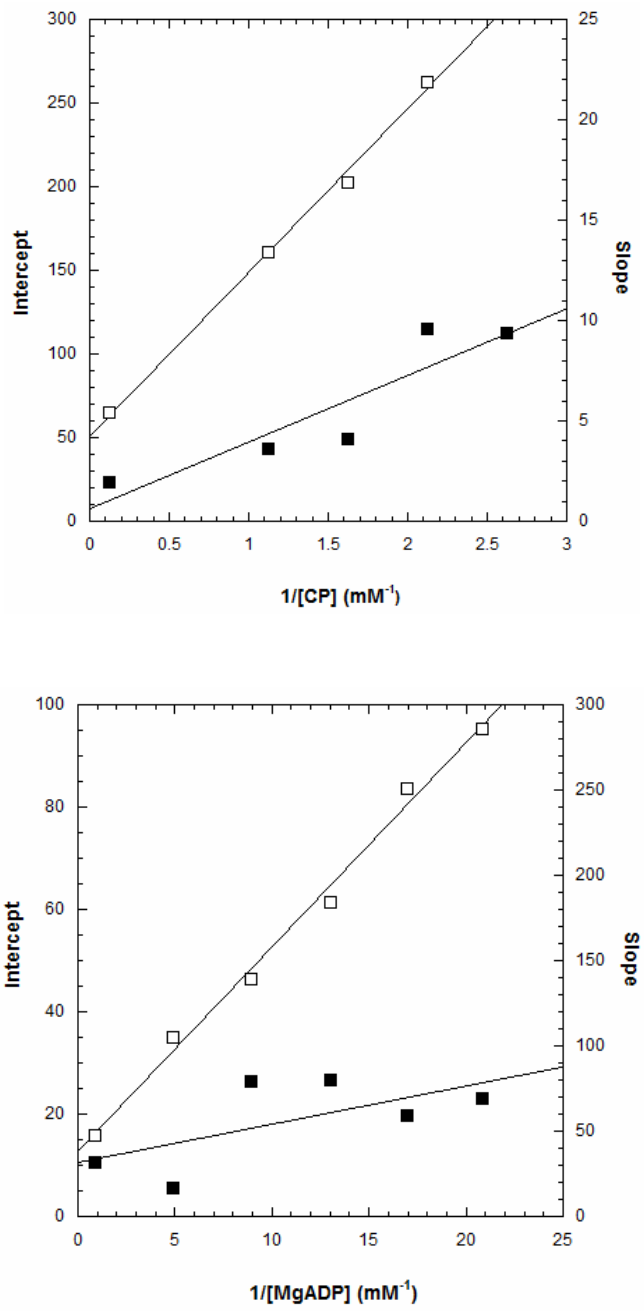

Figure 12: Secondary plots of Slope and Intercept values for large subunit experiments: Top) Secondary plot of the Slope and intercept values from the primary plot in which MgADP was varied at fixed concentrations of CP. closed squares- Intercept, open squares-Slope. Bottom) Secondary plot of the Slope and intercept values from the primary plot in which CP was varied at fixed concentrations of MgADP. Closed squares- intercept, open squares- slope.

Enzyme Form	Rate Equation	K_{ia}(mM)	K_a(mM)	K_b (mM)	k_{cat}(sec^{-1})
Heterodimer	Steady-state sequential	0.20 ±0.03	0.016 ±0.002	0.66 ±0.06	0.27 ±0.01
	Equilibrium Ordered	0.5 ±0.1	N/A	0.36 ±0.07	0.246 ±0.005
Large Subunit	Steady-state sequential	0.25 ±0.08	0.42 ±0.06	2.4 ±0.4	0.06 ±0.01
	Equilibrium Ordered	0.086 ±1.5	N/A	0.025 ±0.4	0.04 ±0.01

Table 1: Extrapolated parameters from initial velocity studies for both enzyme species studied. Data sets were fit to equations 2 and 3 for steady-state sequential and equilibrium ordered mechanisms, respectively using IgorPro multivariate analysis software.

Discussion

In this work, CPS was expressed and purified both as a heterodimer and large subunit (product of the *carB* gene). Initial velocity kinetic studies conducted illustrate that the kinetic mechanism for the ATP synthesis reaction of CPS is sequential, similar to previously published data[20].However, previously published work suggested that the kinetic mechanism for the ATP synthesis reaction proceeded through an equilibrium ordered mechanism. These data, presented here, are in agreement with literature that a sequential mechanism best describes the ATP synthesis reaction. However, the data does not support the conclusion of an equilibrium ordered mechanism. The values obtained for V_m, K_{ia}, from fitting data from the heterodimer experiments to Equation 2 are in agreement with previously published results[20]. K_b and K_a demonstrate divergence from previously reported values. In this report $K_a$is determined to be 16 µM for the heterodimer while previous work has suggested that K_a is zero also; K_b was experimentally determined to be 656 µM compared to a literature value of 1.5 mM[20].

Since previous work reported the heterodimer exhibited unusual mechanistic characteristics, an investigation of the mechanism for the large subunit in isolation was undertaken to determine if the liberation of the subunit interface had an impact on the kinetic mechanism. Inspection of the double reciprocal plots for the large subunit (Figure 11) clearly demonstrates a deviation from the behavior seen in the plots for heterodimer (Figure 9) as the extrapolation to the intersection points in Figure 11 are displaced from those found in Figure 9.

The kinetic parameters extracted from a multivariate fit of the data also support a significant change to the binding constants in the kinetic mechanism. The large subunit in isolation exhibits a 26-fold increase in the Michaelis constant for MgADP and a 3.6 fold increase in the Michaelis constant for CP compared to the heterodimer. Interestingly, the thermodynamic dissociation constant for MgADP, K_{ia} , is not significantly different between the enzyme species. Both data sets for the heterodimer and the large subunit are best described by Equation 3, which implies that there is a sequential addition of substrates to the enzyme but do not indicate an obligatory order to the addition of substrates.

Fitting the data for the large subunit experiments to Equation 3, representing the sequential mechanism seen in the heterodimer, yields values with low error. Equation 3 describes steady-state ordered and steady-state random kinetic mechanisms and contains Michaelis constants for both substrates in the denominator, K_a and K_b. As seen in Table 1, fitting the data from the large subunit experiments to the symmetric rate Equation returns a non-zero value for K_a. In light of the pattern exhibited in the reciprocal plots and the non-zero value for the Michaelis constant of MgADP; we conclude that the liberation of the subunit interface has caused a significant increase in the Michaelis constant but not the thermodynamic dissociation constant of MgADP in the ATP synthesis reaction of wild type CPS. In order to determine the exact nature of the kinetic mechanism more experimentation will be needed.

CHAPTER IV

QUANTIFICATION OF THE ACTIVATION BY ORNITHINE IN LARGE SUBUNIT OF CARBAMOYL PHOSPHATE SYNTHETASE

Introduction

Carbamoyl phosphate synthetase (CPS) is a heterodimeric protein in *E. coli*. It catalyzes the formation of carbamoyl phosphate from bicarbonate, two equivalents of MgATP and a nitrogen source (Glutamine in vivo). The enzyme, as a heterodimer, makes use of three separate yet concerted reaction centers[63,44]. The three reaction centers catalyze partial reactions using the aforementioned substrates in the following way.

(1) $$L - Glutamine \rightarrow NH_3 + L - Glutamate$$

(2) $$NH_3 + HCO_3^- + MgATP \rightarrow Carbamate + MgADP + P_i$$

(3) $$Carbamate + MgATP \rightarrow Carbamoyl\ Phosphate + MgADP$$

(4) $$Carbamoyl\ Phosphate + MgADP \rightarrow Carbamate + MgATP$$

(5) $$HCO_3^- + MgATP \rightarrow MgADP + P_i$$

Reaction (1) is catalyzed by the smaller, 42 kDa, subunit and provides the ammonia needed for reaction (2). To facilitate the catalysis at the second reactive site the ammonia ion is directed via an intramolecular tunnel to its destination. The tunnel allows for sequestering of the diffusible ammonia as well as providing a coordination mechanism for the delivery of the ammonia to the second reactive site where the bicarbonate that has been activated via phosphorylation is then amidated [72,77–79]

Previous studies have demonstrated the viability of all three reactions when interrogated as individual catalytic centers[44,43]. Also, established by Trotta in 1974 is the

preservation of an allosteric response in the ATP synthesis reaction of isolated large subunit[58]. Trotta's work demonstrated that both the activation by ornithine and the inhibition by UMP was preserved. However, the group did not extensively investigate the allosteric response, only confirmed its preservation upon dissociation of the heterodimeric CPS.

The allosteric response of heterodimeric CPS was exhaustively studied by Braxton et al. in the 1990's. Her work using initial velocity kinetics characterized the nature and magnitude of each allosteric ligand in relation to; glutamine dependent CP synthesis, bicarbonate dependent ATPase, and ATP synthesis[20]. In addition to the characterization of the allosteric response Braxton later published results that quantified the interplay between allosteric ligands that can bind simultaneously at different sites[31]. These data demonstrated the dominance of ornithine activation when the inhibitor UMP is present in saturating concentrations. In yet another communication, Braxton reported that the allosteric response engendered by ornithine and UMP is dominated by the entropic component, $T\Delta S_{ax}$ of the coupling free energy, ΔG_{ax}[56].

The trade-off between the loss of entropy and gain of enthalpic stability from bond formation is central to many biological processes. The difference in the thermodynamic parameters ΔH and $T\Delta S$ provide a measure of the propensity of a process to be favorable or non-favorable through the measure of Gibb's free energy. In biological processes, there are often entropic penalties to a process; $T\Delta S$ is less than zero, as the system becomes more ordered. In order for such a process to be favorable, the value of the enthalpy component, ΔH, must compensate for the unfavorable $T\Delta S$

term. This compensation will result in a negative ΔG value which is indicative of a favorable (Equation 1) and enthalpy driven process. However, cases do occur where the process is dominated by a positive, favorable, $T\Delta S$ term. In these cases, one being the allosteric regulation of CPS, the absolute value of the $T\Delta S$ term is larger than a potentially, but not always unfavorable, value of the ΔH term. This situation results in an entropy driven process.

(1) $$\Delta G = \Delta H - T\Delta S$$

In more specific terms for this communication, we express a free energy for the coupling between the binding of allosteric ligand and enzyme substrate. In order to explore the thermodynamics of the allosteric response we will interrogate the system using steady-state kinetics and relate the quantification of the allosteric coupling to an equilibrium constant.

The system we choose to employ here is modeled in Scheme 3. A single-substrate, single-modifier scheme in which the free enzyme, E, can bind either ligand A or effector X. Upon binding, the now binary complex is capable of binding the second ligand. Both of these pathways result in an enzymatically competent ternary complex with effector X and substrate A bound to the enzyme.

$$
\begin{array}{ccc}
E + A & \overset{K_{ia}^{0}}{\rightleftharpoons} & EA \longrightarrow E + P \\
+ & & + \\
X & & X \\
K_{ix}^{0} \uparrow\downarrow & & \uparrow\downarrow K_{ix}^{\infty} \\
XE + A & \underset{K_{ia}^{\infty}}{\rightleftharpoons} & XEA \longrightarrow E + P
\end{array}
$$

Scheme 3: A Single-substrate, single-modifier system in which free enzyme, E, can bind substrate, A, or effector, X. Subsequent binding of the alternative ligand results in a catalytically competent ternary complex XEA.

In this scheme, if the rapid equilibrium assumption is valid, a determination of $K_{1/2}$ will also yield the value for K_{ia}^{0}. K_{ia}^{0} is the thermodynamic dissociation constant for enzyme substrate complex in the absence of effector. Following this pathway in the scheme, one can titrate in effector X and determine $K_{1/2}^{app}$, representing the apparent dissociation constant for A at known concentrations of X. These data are then fit to Equation 2 which allows the extraction of K_{ia}^{0}, K_{ix}^{0} and Q_{ax}.

(2) $$K_{1/2}^{app} = K_{ia}^{0}\left(\frac{K_{ix}^{0}+[X]}{K_{ix}^{0}+Q_{ax}[X\}}\right)$$

These data, simulated in Figure 13, give a graphical indication of the saturable nature of an allosteric ligand's effect and provide the basis on which Q_{ax} is determined. The value Q_{ax} provides a quantitative measure of the impact an allosteric effector engenders on the binding of substrate as described by Reinhart[35]. As described by Reinhart, the ratio of the

dissociation constants K_{ia}^{0} to K_{ia}^{∞} is equal to the coupling quotient, Q_{ax}. Furthermore, through substitution and simple algebraic rearrangement of equations 3-5, it is seen that Q_{ax} is an equilibrium constant for a for reaction scheme which represents the ligand bound enzyme states in Equation 6.

(3) $$Q_{ax} = \frac{K_{ia}^{0}}{K_{ia}^{\infty}} = \frac{K_{ix}^{0}}{K_{ix}^{\infty}}$$

(4) $$K_{ia}^{0} = \frac{[E][A]}{[EA]} \qquad K_{ia}^{\infty} = \frac{[A][XE]}{[XEA]}$$

(5) $$Q_{ax} = \frac{[E][XEA]}{[EA][EX]}$$

(6) $$EA + XE \overset{Q_{ax}}{\longleftrightarrow} E + XEA$$

Through the use of these identities and the establishment of Q_{ax}as an equilibrium constant for the disproportionation equilibrium, the thermodynamic components of the allosteric effect of a ligand can be determined via Van't Hoff analysis.

Presented here is evidence that the liberation of the subunit interface of wild type CPS from *E. coli* affects the entropic component of allosteric activation by ornithine in both the bicarbonate dependent ATPase and ATP synthesis partial reactions. Also, emerging from the data presented is the observation that a larger increase in the entropic contribution is seen in the reaction center most proximal to the liberated interface.

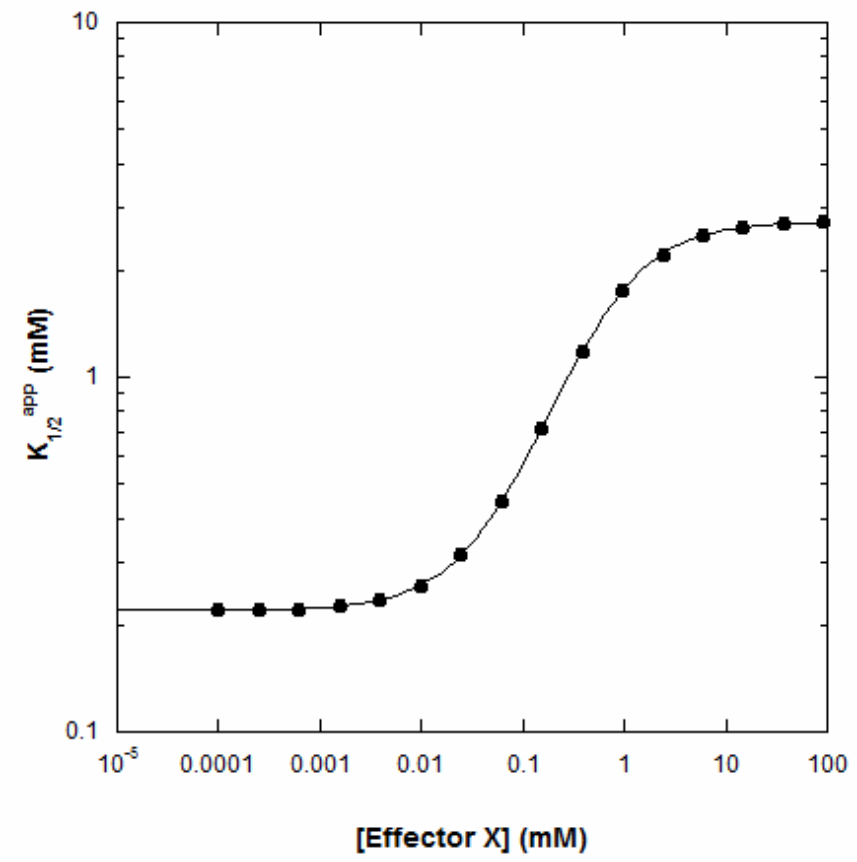

Figure 13: Simulated data of $\boldsymbol{K_{1/2}^{app}}$ for substrate A as a function of effector X. The data demonstrate a lower plateau which when extrapolated to the abscissa marks the $\boldsymbol{K_{ia}^{0}}$ and an upper plateau which denotes the $\boldsymbol{K_{ia}^{\infty}}$. The logarithm of the difference between the plateaus provides a quantification of the nature and magnitude of the allosteric effect, $\boldsymbol{Q_{ax}}$. These data represent inhibition as $\boldsymbol{K_{ia}^{0}}$is less than $\boldsymbol{K_{ia}^{\infty}}$.

Results

Bicarbonate Dependent ATPase Reaction

The active site for bicarbonate dependent ATPase activity of CPS is located entirely within the large subunit of CPS[80]. Bicarbonate activation by MgATP is the second partial reaction of the synthesis of CP using glutamine as a nitrogen source. Establishing the behavior of the heterodimer and the large subunit in isolation with respect to each active site is critical elucidation of the underlying thermodynamics of allosteric regulation of the enzyme. The heterodimer and the large subunit of CPS in isolation are active and follow Michaelis–Menten kinetics as evident from the hyperbolic dependence of specific activity on the concentration of substrate, MgATP (Figure 14). The concentration of HCO_3^- was saturating at 10 mM through the addition of $KHCO_3$. There are evident differences in the kinetic constants for the bicarbonate dependent ATPase activity of heterodimeric and the large subunit of CPS. The heterodimer has a specific activity of 0.085 ±0.002 U/mg while the large subunit in isolation exhibits a specific activity of 0.021± 0.001 U/mg, only 25% of the activity exhibited by the heterodimer.

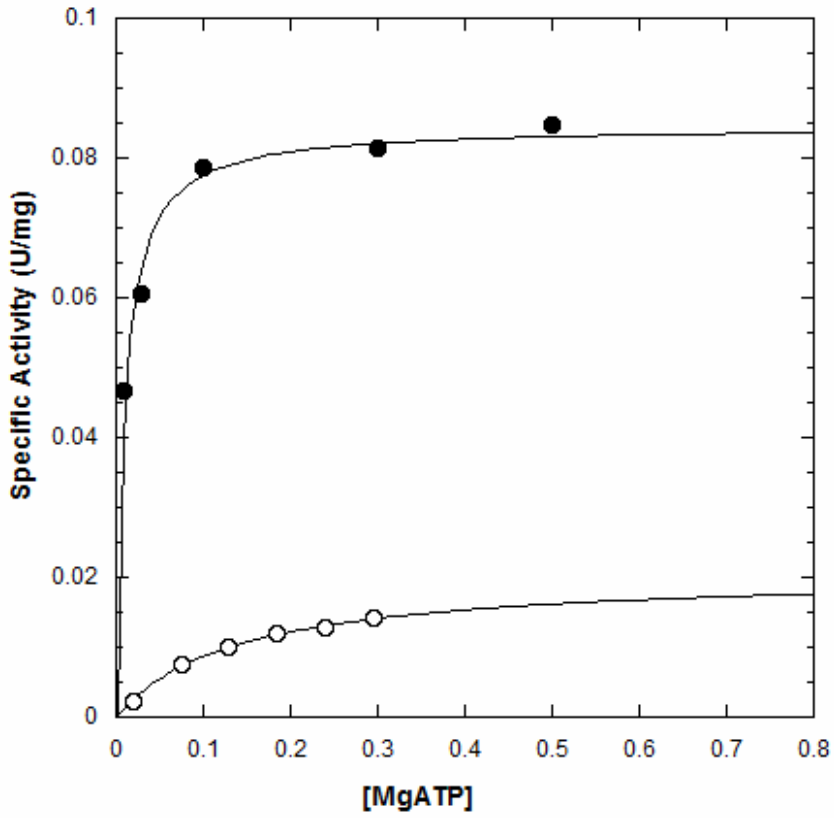

Figure 14: Initial velocities of bicarbonate dependent ATPase activity in CPS heterodimer (closed circles) and large subunit (open circles) as a function of MgATP. Reactions contain saturating bicarbonate at 10 mM.

Determination of the K_m for MgATP while titrating the concentration of the allosteric activator L-ornithine provides evidence of a relationship between K_m and ornithine in both the heterodimer and the large subunit in isolation (Figure 15). The data from Figure 15 suggest that the thermodynamic dissociation constant, K_{ia}^0, in the heterodimer and the large subunit in isolation are, 7 ±2 μM and 150 ±20 μM respectively. The dissociation constant representative of effector binding, K_{ix}^0, in the large subunit is 245 ±65 μM. The qualitative difference in the enzyme species is quite apparent.

In order to obtain more robust fitting of the large subunit data to Equation 2 the K_{ix}^0 determined from the ATP synthesis reaction with the large subunit was used as a fixed parameter. K_{ix}^0, is the dissociation constant for ornithine in the absence of any other ligand and is the same regardless of which reaction or substrates may be titrated in experimentation. K_{ix}^0 determined from the ATP synthesis reaction exhibited less error than K_{ix}^0 determined with the ATPase reaction.

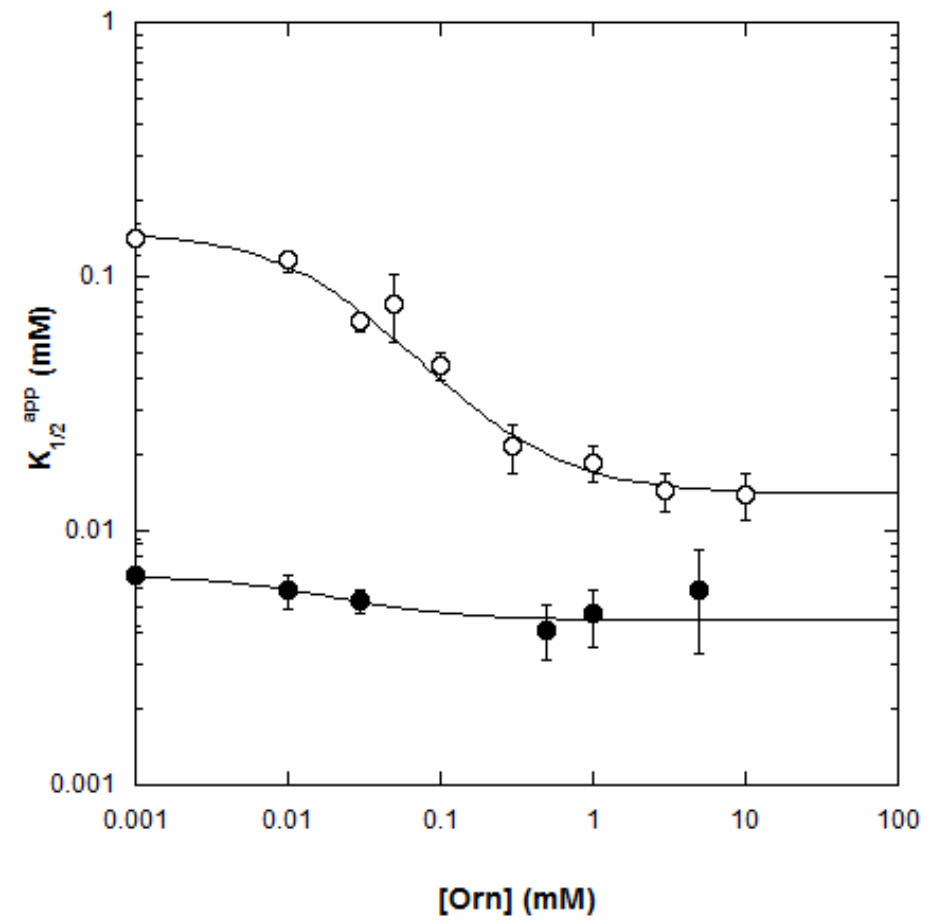

Figure 15: Plot of apparent dissociation constant for MgATP as a function of ornithine for the bicarbonate dependent ATPase reaction of CPS. Closed circles represent heterodimeric CPS, open circles represent the large subunit in isolation.

Also, apparent from the data is that the value of Q_{ax}, the measure of allosteric coupling, at a temperature of 298K is increased when the large subunit is interrogated in isolation, 10 ±1, when compared to the Q_{ax} of the heterodimer 1.5 ±0.5. This increase in the value of Q_{ax} indicates a stronger activation effect on MgATP binding by ornithine in the large subunit in isolation.

Investigation of the thermodynamic components of the allosteric coupling requires determination of Q_{ax} at various temperatures. The heterodimer displayed no significant response to variation in temperature from 288K to 308K (Figure 16 bottom). The value of Q_{ax} at these temperatures is approximately 2, indicating that ornithine has a very modest effect on MgATP binding in this reaction center.

The large subunit in isolation demonstrated a significant increase in Q_{ax} at all temperatures examined when compared to the heterodimer, consistently 10 ±1 (Figure 16 Top). The large subunit in isolation demonstrated the same modest response to changes in temperature as the heterodimer between temperatures of 288K and 308K.

Of additional interest is the values of K_{ia}^{0} as a function of temperature. The K_{ia}^{0} decreases as the temperature is decreased. I speculate that this is due to increased stability of the active site. The bicarbonate dependent ATPase reaction center is directly adjacent to the liberated interface. This may cause instability in the active site that is offset at lower temperatures.

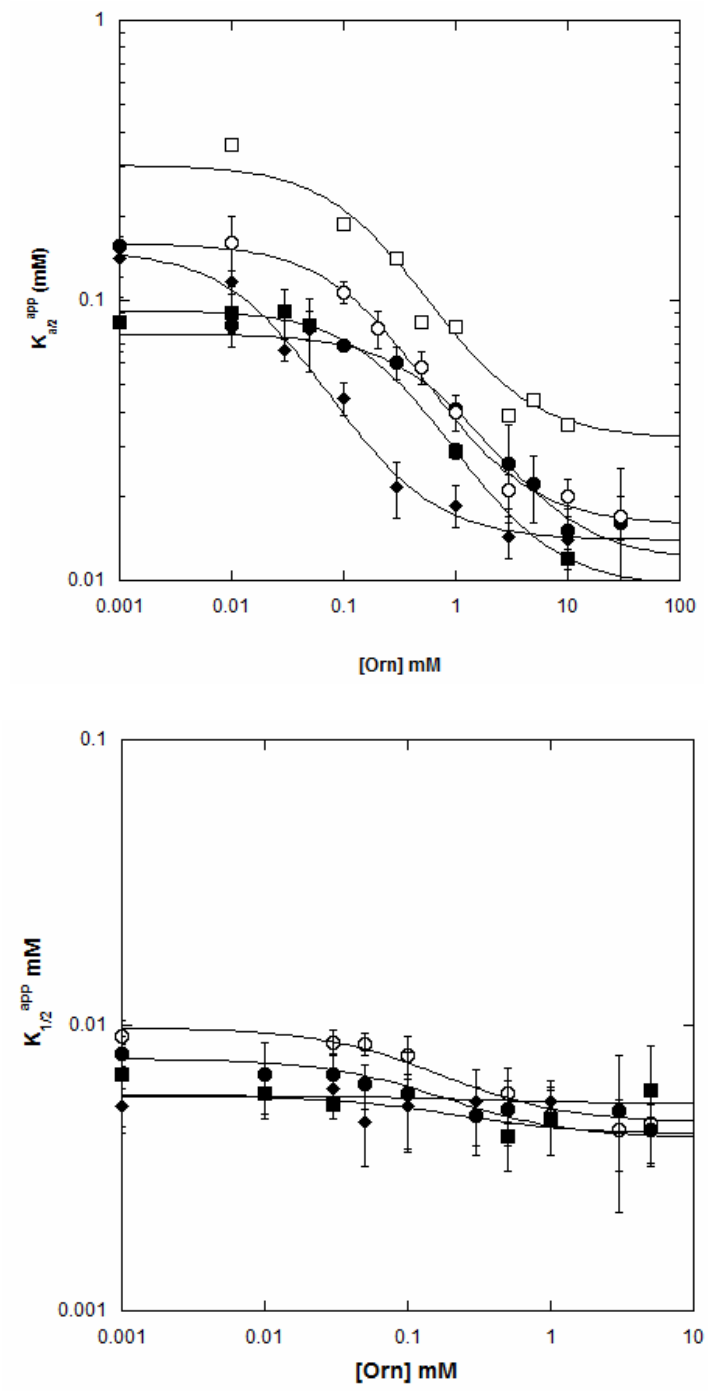

Figure 16: $K_{1/2}$ as a function of ornithine concentration for the bicarbonate dependent ATPase reaction of CPS at varied temperatures. Top panel represents large subunit data; bottom panel displays Heterodimeric data. (●- 288K, ■- 293K, ♦- 298K, ○- 303K, □- 308K)

Since Q_{ax} is the equilibrium constant for the disproportionation equilibrium, Van't Hoff analysis was performed on the temperature dependence of Q_{ax}(Figure 17). This allows the extraction of the thermodynamic components of the Gibb's free energy associated with the allosteric activation of MgATP binding at the bicarbonate dependent ATPase reaction site. Inspection of Figure 17 indicates that the allosteric phenomenon is entropically dominated; the slope of both trend lines is negative resulting in a positive value for ΔH_{ax}. Using the determination of Q_{ax} at 298K, ΔG_{ax} is calculated using Equation 7. ΔH_{ax} is determined from the slope of the trend line in Figure 17 for the respective enzyme species. The value of $T\Delta S_{ax}$ is then solved for algebraically through Equation 1. The extracted values are presented in Table 2.

(7) $$\Delta G_{ax} = -RT \ln(Q_{ax})$$

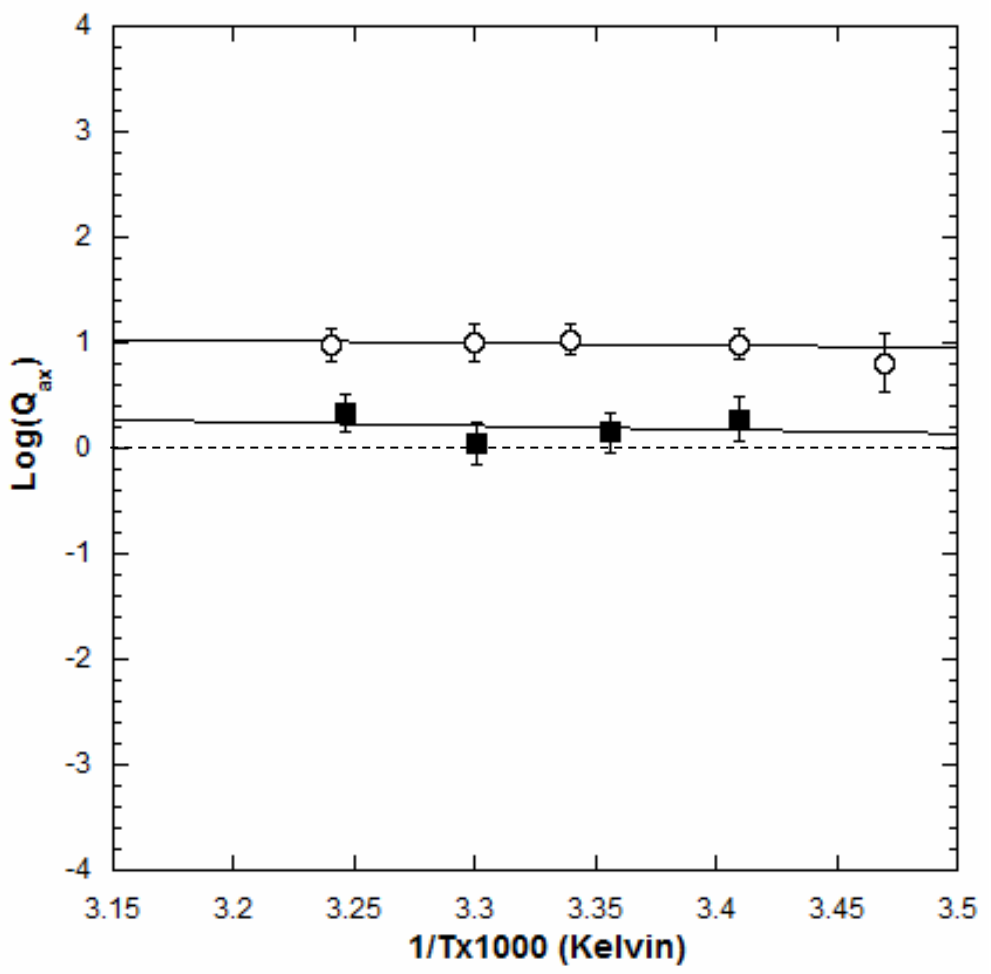

Figure 17: Van't Hoff analysis of the coupling between MgATP and ornithine with respect to the bicarbonate dependent ATPase reaction of CPS. Plot is the logarithm of the coupling parameter $\boldsymbol{Q_{ax}}$ as a function of inverse temperature in Kelvin. Closed squares represent the heterodimer and open circles represent the large subunit in isolation.

Enzyme Species	ΔH_{ax} (cal/mol)	$T\Delta S_{ax}$ (kcal/mol)	ΔG_{ax} (kcal/mol)
Heterodimer	1 ± 1	0.2± 0.1	-0.2 ± 0.1
Large subunit	0.6 ± 0.4	1.42 ± 0.05	-1.42 ± 0.05

Table 2: Thermodynamic components of the Gibb's free energy associated with the allosteric activation of MgATP binding by ornithine extracted from the linear fit of the data in Figure 17.

ATP Synthesis Reaction

The active site for synthesis of ATP from MgADP and carbamate is removed from the subunit interface by 45 Å and is immediately proximal to the allosteric binding domain of CPS. In fact, Thoden et al. demonstrated that ornithine binds residues in both allosteric and the carbamoyl phosphate synthesis domains[81]. These factors lead one to believe that liberation of a subunit interface distal to the active and allosteric sites would engender minimal perturbation to the system. Following is evidence that liberating the subunit interface substantially impacts the binding of ornithine and the magnitude of the allosteric effect yet, does not significantly affect the binding constant K_{ia}^{0}.

As in the bicarbonate dependent ATPase reaction, the hyperbolic dependence of specific activity on substrate concentration with respect to ATP synthesis is preserved when the large subunit is interrogated in isolation.

As stated previously, ornithine binds proximal to the ATP synthesis active site and is 45 Å distal to the subunit interface. An initial confirmation of the preservation of allosteric control of the ATP synthesis reaction by ornithine was conducted at 298K with both enzyme constructs (Figure 18). While activation by ornithine is evident in both data sets, the large subunit demonstrates attenuated activation and slightly decreased affinity for MgADP compared to heterodimeric CPS. The plateau in the Figure 18 occurring at low ornithine concentrations can be extrapolated to the y-axis and provides the dissociation constant for MgADP in the absence of ornithine. The K_{ia}^{0} for the heterodimer and the large subunit are 0.30 ± 0.02 mM and 0.325 ± 0.002 mM,

respectively. Similarly, Q_{ax}, the quantitation of the nature and magnitude of the allosteric effect, is 18 ± 5 for the heterodimer and 4.6 ± 0.5 for the large subunit alone.

Following confirmation of allosteric response at 298K, Q_{ax} was determined at temperatures ranging from 288K to 308K at 5K intervals. Depicted in Figure 19 are overlays of the $K_{1/2}$ as a function of ornithine concentration at the various temperatures for the heterodimer and the large subunit.

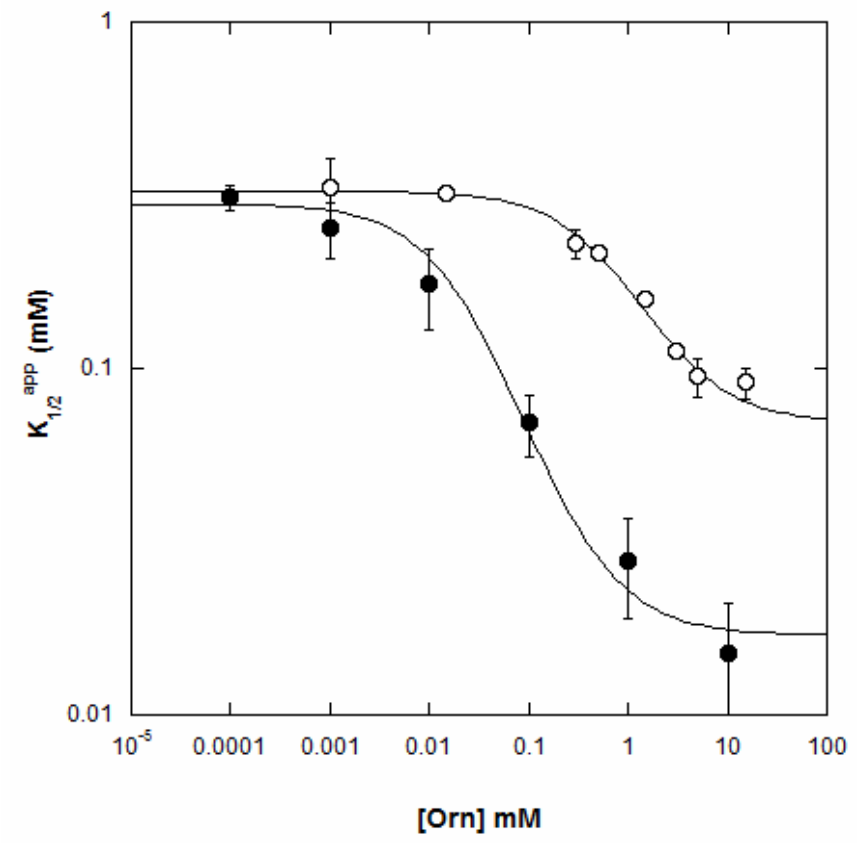

Figure 18: Plot of apparent dissociation constant for MgADP as a function of ornithine for the ATP synthesis activity in CPS. Heterodimer (closed circles), large subunit (open circles) at 298K.

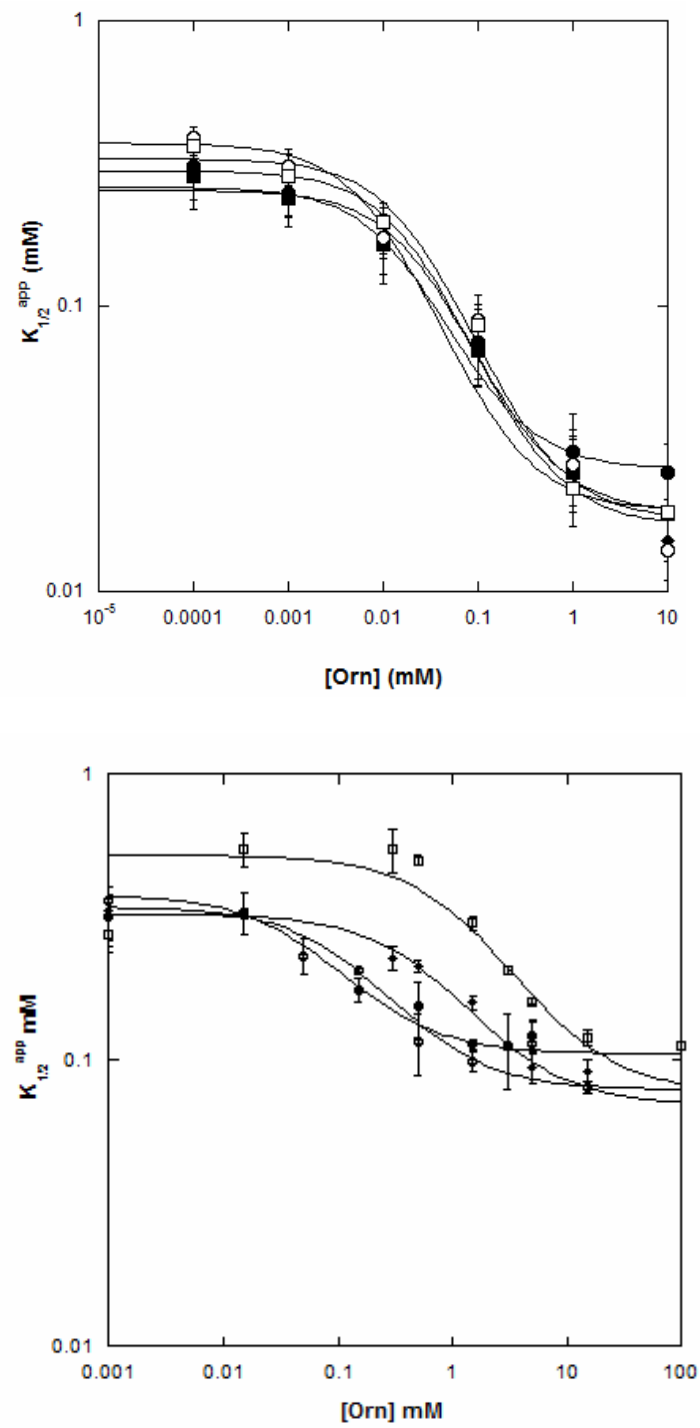

Figure 19: $K_{1/2}$ as a function of ornithine concentration at varied temperatures for the ATP synthesis reaction of CPS. Top panel represents heterodimer data; bottom panel displays large subunit data. (●- 288K, ■- 293K, ♦- 298K, ○- 303K, □- 308K)

Using the same methodology applied to the bicarbonate dependent ATPase reaction, Van't Hoff analysis was performed on the temperature dependence of ornithine activation in the ATP synthesis reaction. Figure 20 demonstrates the dependence of the allosteric response as a function of temperature. Strikingly, these data are remarkably similar between the heterodimer and the large subunit. Both trend lines have a negative slope leading to a positive ΔH_{ax}. Considering the ΔG_{ax} at 298K for heterodimer and large subunit is -1.71 ± 0.02 kcal/mol and -0.91 ± 0.06 kcal/mol, respectively, it is evident that the allosteric effect of ornithine is entropically driven. The slope of each trend line is used to calculate ΔH_{ax} for each enzyme species, 0.6 ± 0.1 cal/mol and 0.8 ± 0.3 cal/mol, as before. Values for $T\Delta S_{ax}$ are solved for algebraically using equation 1. The thermodynamic values are enumerated in Table 3.

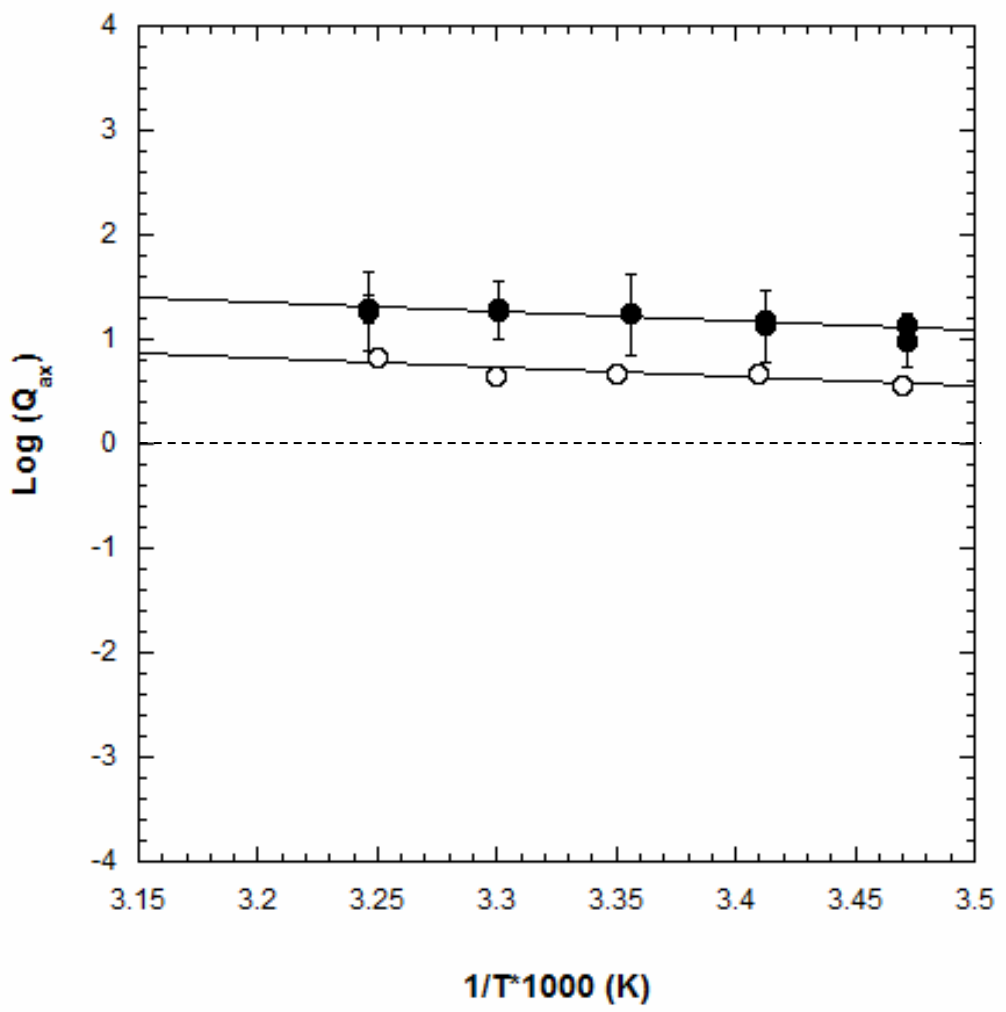

Figure 20: Van't Hoff analysis of the coupling between MgADP and ornithine with respect to the ATP synthesis reaction of CPS. Plot is the logarithm of the coupling parameter $\boldsymbol{Q_{ax}}$ as a function of inverse temperature in Kelvin. Closed circles represent the heterodimer and open circles represent the large subunit in isolation. When not visible, error bars are smaller than the symbol.

Enzyme Species	ΔH_{ax} (cal/mol)	$T\Delta S_{ax}$ (kcal/mol)	ΔG_{ax} (kcal/mol)
Heterodimer	0.6 ± 0.1	1.71 ± 0.02	-1.71 ± 0.02
Large subunit	0.8 ± 0.3	0.91 ± 0.06	-0.91 ± 0.06

Table 3: Thermodynamic components of the Gibb's free energy associated with the allosteric activation of MgADP binding by ornithine extracted from the linear fit of the data in Figure 21.

Discussion

The thermodynamic principles at work in any process are critical to its understanding. Here we have investigated the thermodynamics of the allosteric regulation of *E. coli* CPS by ornithine utilizing both the bicarbonate dependent ATPase and the ATP synthesis partial reactions. Through the removal of the glutaminase subunit of the heterodimeric native enzyme, we sought to increase the intrinsic conformational entropy of the large subunit to investigate the impact on the allosteric coupling in CPS. We found that the two partial reactions respond to the liberation of the subunit interface in different manners.

The 1.1 kcal/mol decrease in ΔG_{ax} at 298K with respect to the bicarbonate dependent ATPase reaction indicates that the allosteric effect of ornithine is augmented by the liberation of the subunit interface. Van't Hoff analysis of the allosteric coupling quotient Q_{ax} allowed for determination of the entropic and enthalpic components of the ΔG_{ax}. The enthalpic component of the free energy of coupling, ΔH_{ax}, between MgATP and ornithine is decreased by 0.4 cal/mol at 298K while the absolute value of entropic component, $T\Delta S_{ax}$, is increased by 1.2 kcal/mol. These data suggest that the increase in entropy associated with binding of ornithine to CPS is increased when the glutaminase subunit is removed relative to the entropy associated with ornithine binding to the heterodimer. As the allosteric response is entropy dominated, the dramatic increase in activation of the large subunit by ornithine compared to the heterodimer further supports the conclusion that the liberation of the interfacial restraints impacts the entropy of the allosteric coupling between MgATP and ornithine. The bicarbonate dependent ATPase

active site is in close proximity to the liberated interface and as such provides a structural basis for suggesting the reaction center would be strongly subject to any perturbation afforded by the liberation of the interface. It stands to reason that the decreased conformational restraints experienced by the large subunit have augmented the $T\Delta S_{ax}$ term of ΔG_{ax} and resulted in the increased activation of the reaction by ornithine.

By contrast, the active site for synthesis of ATP is spatially removed from the subunit interface by 45 Å and is situated directly next to the allosteric binding site for ornithine. These conditions would lead one to conclude that there is not a great impact on the ATP synthesis reaction upon liberation of the subunit interface. Indeed, there is only a very modest impact on the $K_{1/2}$ for MgADP. However, upon investigation of the allosteric response, there is an attenuation of the activation by ornithine when the subunit interface is liberated.

Our working hypothesis was that the increased conformational freedom would impact the $T\Delta S_{ax}$ term of the free energy and result in a perturbation to the coupling quotient. The decrease of Q_{ax} at 298K from 18 to 4.6 upon liberation of the subunit interface was surprising although not outside the realm of possibilities. Interestingly, as the activation of the ATP synthesis reaction was reduced by 75% there was no significant change in the thermodynamic dissociation constant K_{ia}^{0}, approximately 350 μM for each enzyme species. The lack of change in the dissociation constant considered in tandem with the change in the coupling quotient suggest that the difference arises

from a breakdown of the communication network for the allosteric signal as opposed to a change in structural orientations of the active site residues.

The slopes of the trend lines are very shallow and as such, the ΔH_{ax} component in the coupling free energy of either enzyme construct is less than 0.001 kcal/mol while at 298K $T\Delta S_{ax}$ for the heterodimer and the large subunit is 1.71 kcal/mol and 0.91 kcal/mol, respectively.

Initially this result appears inconsistent with the liberation of the subunit interface generating an increase in the entropy of the enzyme. However, one must consider the disproportionation equilibrium when discussing the impact of the allosteric effector. With respect to the heterodimer, the binding of ornithine shifts the equilibrium to favor the XEA complex with both the substrate and the effector bound. When the large subunit is interrogated in isolation the entropy of all four species in the disproportionation equilibrium are impacted, to potentially varying degrees, by the loss of the interfacial restraints. In the case of ATP synthesis activation by ornithine, the data suggests that the disproportionation equilibrium has been shifted to the left, favoring the binary complexes of XE and EA, as a result of the increased entropy. This is not a contradictory result as all four complexes in the disproportionation equilibrium can respond to the reduced interfacial restraints in a unique manner.

Results presented here indicate that the bicarbonate dependent ATPase reaction of CPS is more profoundly affected by the removal of the glutaminase subunit than the ATP synthesis reaction. This is evident from the large change in Michaelis constant in the bicarbonate dependent ATPase reaction and the negligible change of the K_{ia}^{0} in the

ATP synthesis reaction. The allosteric activation by ornithine is also an indicator of the differential effect of liberating the subunit interface. With respect to the bicarbonate dependent ATPase reaction these data demonstrate an increased activation and a resultant ΔG_{ax} decrease of 1.1 kcal/mol compared to the observed increase of 0.6 kcal/mol in ΔG_{ax} with respect to ornithine in the ATP synthesis reaction.

The thrust of this investigation is to interrogate the entropic component of the allosteric activation of CPS by ornithine. The results provide answers while raising more questions. The removal of conformational constraints through the liberation of the subunit interface is intended to elevate the entropy associated with the enzyme as a whole and thereby demonstrate an impact on activation by ornithine through the enrichment of the entropic component of ΔG_{ax}. These results suggest that in regard to the bicarbonate dependent ATPase reaction as the $T\Delta S_{ax}$ term is increased by 1.1 kcal/mol and the coupling quotient, Q_{ax}, is increased 5-fold while the enthalpic component remains constant between the enzyme constructs. However, the ATP synthesis reaction demonstrates a surprising reduction in the $T\Delta S_{ax}$ component of 0.6 kcal/mol when the interface is liberated. The decrease in $T\Delta S_{ax}$ results in a 75% decrease in the Q_{ax} of for the large subunit compared to the heterodimer, indicating a significant reduction in activation by ornithine. The impact demonstrates that ΔS_{ax} derives from conformational entropy and is not an effect of solvation.

CHAPTER V

UMP INHIBITION IS SIGNIFICANTLY PERTURBED UPON LOOSENING OF INTERFACIAL RESTRAINTS

Introduction

Carbamoyl Phosphate Synthetase (CPS), a heterodimeric enzyme, plays a pivotal role in the de novo synthesis of pyrimidine nucleotides by synthesizing the compound, carbamoyl phosphate, which provides the N_3 and C_2 of the pyrimidine ring (Figure 21).

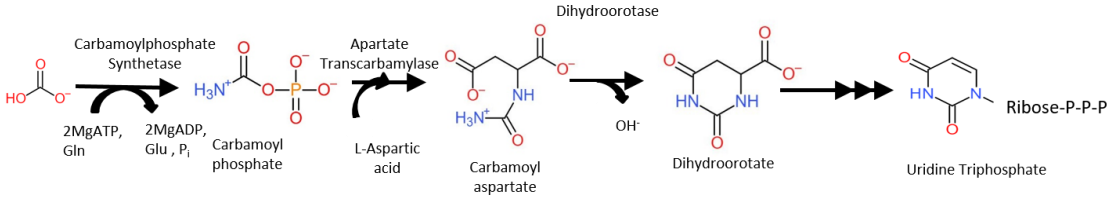

Figure 21: Initial steps of pyrimidine biosynthesis demonstrating the incorporation of CP into the heterocyclic ring of the nitrogenous base.

As such, CPS exhibits allosteric feedback inhibition by the downstream product, UMP. The product of the reaction catalyzed by CPS results in the high energy product carbamoyl phosphate which, when combined with aspartate by the enzyme aspartate transcarbamylase produces carbamoyl aspartate[82]. The carbamoyl aspartate is cyclized by dihydroorotase forming the heterocyclic compound and precursor to pyrimidine nucleotides, dihydroorotate[83].

As discussed in previous chapters, CPS contains three catalytic sites each of which is capable of catalyzing the partial reactions that culminate in the formation of

carbamoyl phosphate[84–87]. The partial reactions of CPS (Reactions 2-4) are located in distinct regions of the enzyme and diffusible or reactive products of one reaction center are ushered to the following reaction center via a 96 Å intramolecular tunnel. The intramolecular tunnel serves two purposes in CPS: 1. to sequester reactive and diffusible intermediates from bulk solvent, and 2. Assist in timing the delivery of intermediates to the next reaction center[72,77].

(1) $L-Glutamine\ +2MgATP\ +HCO_3^-\rightarrow\ Carbamoyl\ phosphate+\ L-\ Glutamate\ +2MgADP+P_i$

(2) $L-Glutamine\rightarrow NH_3\ +L-Glutamate$

(3) $HCO_3^-\ +MgATP\rightleftharpoons HCO_3^-+MgADP+P_i$

(4) $Carbamate+MgATP\rightleftharpoons Carbamoyl\ Phosphate+MgADP$

(5) $Carbamoyl\ Phosphate+MgADP\rightleftharpoons Carbamate+MgATP$

In addition to the three activities of CPS, when it is synthesizing carbamoyl phosphate, the final reaction (reaction 4) can operate in the reverse direction (reaction 5) to synthesize MgATP from MgADP and carbamoyl phosphate[85]. The ATP synthesis reaction of CPS has been extensively studied and it has a simpler stoichiometry than the forward reaction of carbamoyl phosphate synthesis (Reaction 1)[86]. The ATP synthesis reaction has also been shown to demonstrate a robust response to allosteric ligands[31,39,84,88].

The bicarbonate dependent ATPase activity (Reaction 3) of CPS when interrogated as a partial reaction is a futile reaction. The result of the catalysis is the

phosphorylation of bicarbonate at the expense of one equivalent of MgATP being converted to MgADP[87]. However, without a nitrogen source provide for the formation of carbamate, the phosphorylated bicarbonate is released from the enzyme and is degraded via hydrolysis to bicarbonate and inorganic phosphate. This reaction center exhibits a modest response to allosteric ligands as described by Braxton et al[20].

The locations of the reaction centers with regard to the allosteric binding sites and the subunit interface also have impact on the research discussed. As evident from the crystal structure (Figure 22), the bicarbonate dependent ATPase reaction center is proximal to the subunit interface while the ATP synthesis reaction center is removed by 45 Å[46]. In direct contrast, the ATP synthesis reaction center is adjacent to the allosteric binding domain while the reaction center for bicarbonate dependent ATPase activity is substantially further away from the binding site for UMP at 33 Å.

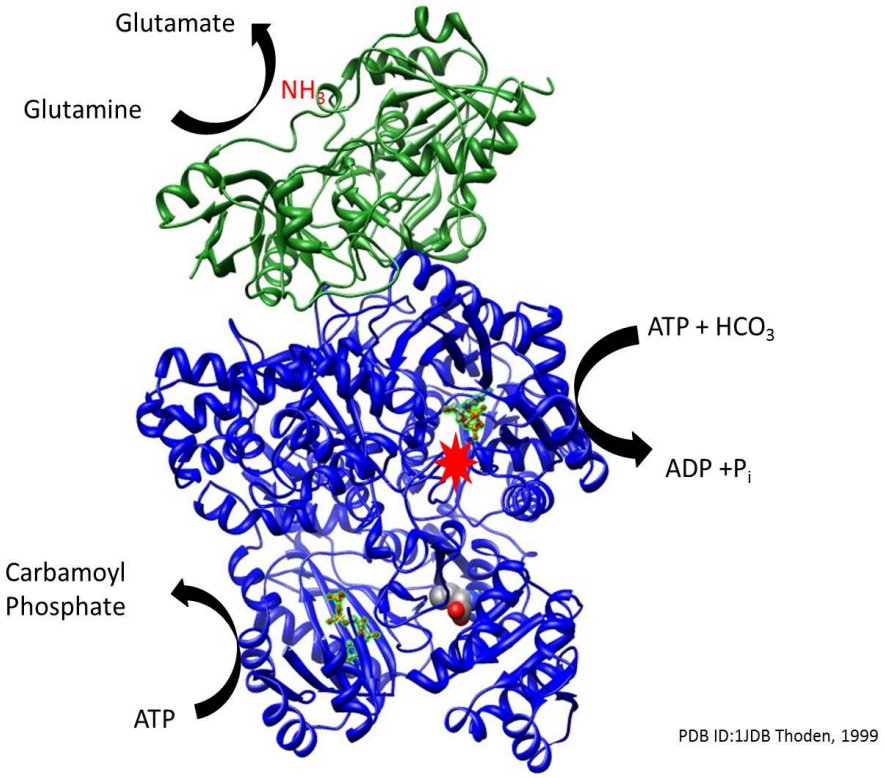

Figure 22: X-ray crystallographic model of heterodimeric CPS. The glutaminase subunit is in green, large subunit in blue. ATP molecules are shown highlighted in ball and stick form and represent the bicarbonate dependent ATPase and ATP synthesis reaction centers as described. Ornithine is shown as a space filled model to denote the allosteric binding domain[49].

Of particular note is work presented by Braxton et al in which Van't Hoff analysis of the allosteric response of heterodimeric CPS in regard to the ATP synthesis reaction demonstrated that the effects of allosteric ligands in CPS are entropy driven[56]. An entropy driven system arises when the absolute value of $T\Delta S$ is larger than that of ΔH and they have the same sign.

Since it has been demonstrated here and in previous reports that the partial reactions of CPS located on the large subunit are still viable when the glutaminase subunit is removed, the large subunit of CPS was expressed and purified in the absence of the

glutaminase subunit. We hypothesize the liberation of the interface will introduce a reduction in conformational restraints to the residues at the interface and possibly augment the entropic contribution to allosteric effects. Presented here, is evidence that the liberation of the subunit interface of CPS has profound effects on the allosteric response to UMP in both the bicarbonate dependent ATPase reaction and the ATP synthesis reaction.

Materials and Methods

Wild type, heterodimer and large subunit, CPS was grown in 1.5L LB/Ampicillin (100 mg/ml) at 37°C for 18 hours. The cells were harvested via centrifugation in a Beckman D4 centrifuge. Cellular pellets were stored at -20°C until purification of protein. Protein purification proceeded as described in the previous chapter. Initial velocity kinetic experiments were conducted using both enzyme constructs.

The rate of ATP synthesis was monitored using a coupled assay system consisting of hexokinase and glucose-6-phosphate dehydrogenase (RPI) that couples the production of ATP by CPS to the conversion of $NADP^+$ to NADPH (Roche). The production of NADPH can be monitored using UV/Vis spectrophotometry at 340nm using a Beckman DU-40 spectrophotometer. Kinetic experiments were conducted in 600 µl final volume containing: kinetics buffer (50 mM HEPES, 10 mM KCl, 20 mM $MgCl_2$, 0.5 mM EDTA), coupling enzymes (4 U Hexokinase, 4 U G6PDH), 10 mM glucose, 2 mM $NADP^+$, and varying concentrations of MgADP and CP (Sigma). Rates were restricted by dilution of enzyme such that no more than 10% of available substrate was consumed. Initial plots were constructed using Kaleidagraph data analysis software (Synergy Inc.) and multivariate fitting was performed with IgorPro multivariate fitting analysis (WaveMetrics). Data were fit to the following initial velocity rate equations 1 and 2. When CP concentration was not a varied the concentration was limited to $\frac{1}{3}K_m$ per reasons previously mentioned in Chapter 2.

(1) $$\frac{v_0}{E_T} = \frac{V_{max}[A]}{K_a + [A]}$$

(2) $$\frac{v_0}{E_T} = \frac{V_{max}[A][B]}{K_{ia}K_b + K_b[A] + K_a[B] + [A][B]}$$

(3) $$K_a^{app} = K_{ia}^0 \left(\frac{K_{iy}^0 + [Y]}{K_{iy}^0 + Q_{ay}[Y]} \right)$$

Bicarbonate dependent ATPase activity was monitored using a coupled enzyme assay of pyruvate kinase and lactate dehydrogenase. The 600 µL reaction volume contained: kinetics buffer (50 mM HEPES, 10 mM KCl, 20 mM $MgCl_2$, 0.5 mM EDTA), coupling enzymes (4 U Pyruvate Kinase, 4 U LDH), 2 mM NADH, 10 mM $KHCO_3$ and varying concentrations of MgATP. Initial velocity data collected over a range of UMP concentrations were fit to Equation 1 to determine $K_{1/2}^{app}$. Secondary plots generated were fit to Equation 3 to determine values of $K_{iy}^0$and, Q_{ay}.

Results

Bicarbonate Dependent ATPase reaction

The bicarbonate dependent ATPase reaction catalyzed by both heterodimeric CPS and the large subunit in isolation is able to be monitored as discussed previously (Chapter 4). In this report, the concentrations of the allosteric inhibitor UMP were varied to determine the impact liberating the subunit interface of the heterodimer has on the allosteric regulation by UMP.

The bicarbonate dependent ATPase reaction center is adjacent to the dimer interface, yet removed from the allosteric site by 33 Å, and catalyzes the hydrolysis of MgATP to MgADP (Reaction 3) when no nitrogen source is present. This reaction proceeds only when bicarbonate is present as the full forward reaction (Reaction 1) of CPS activates bicarbonate through this phosphorylation prior to amidation. Without a nitrogen source present, it is believed that the activation of bicarbonate by phosphorylation results in a futile cycle in which the newly formed carboxyphosphate degrades via hydrolysis back to bicarbonate and inorganic phosphate[44].

These data demonstrate that the bicarbonate dependent ATPase reaction of both the heterodimeric CP and the large subunit of CPS in isolation respond to the allosteric inhibitory signal from UMP binding however, the two enzyme forms exhibit distinct kinetics, magnitude of allosteric response, and enthalpy-entropy compensation of the allosteric response.

Work presented in Chapter IV has demonstrated the catalytic activity is preserved in the bicarbonate dependent ATPase reaction center upon liberation of the

subunit interface. The allosteric inhibition of the ATPase activity also remains upon liberation of the interface although inspection of $K_{1/2}^{app}$ vs. UMP concentration at 25°C (Figure 23). The data in Figure 23 demonstrate deviations in several parameters when large subunit is compared to the heterodimer. These data suggest the thermodynamic dissociation constant for MgATP in the absence of UMP, K_{ia}^{0}, is increased by 4.5 fold when the glutaminase subunit is removed, resulting in a lower affinity. Interestingly, there is a significant shift in the K_{iy}^{0}, the thermodynamic dissociation constant for UMP in the absence of MgATP. At 25°C K_{iy}^{0} for the heterodimer is 3 ± 2 µM. The large subunit in isolation exhibits a 3 order of magnitude increase in K_{iy}^{0} to 8 ± 31 mM; with such large error the value is essentially meaningless. The binding of UMP to the large subunit could not be determined with better precision due to the concentrations of UMP needed to saturation.

The overall magnitude of the allosteric response parameter Q_{ay} is similar between the heterodimer and the large subunit, 0.43±0.07 and 0.43±0.57 respectively. However, the error in the large subunit is, again, larger than the value. When these data are fit to Equation 3 values for K_{ia}^{0}, $K_{iy}^{0}$and, Q_{ay} can be determined and are enumerated in Table 4. The large decrease in the binding affinity for UMP to the large subunit results in difficulty interpreting the allosteric response at 25°C.

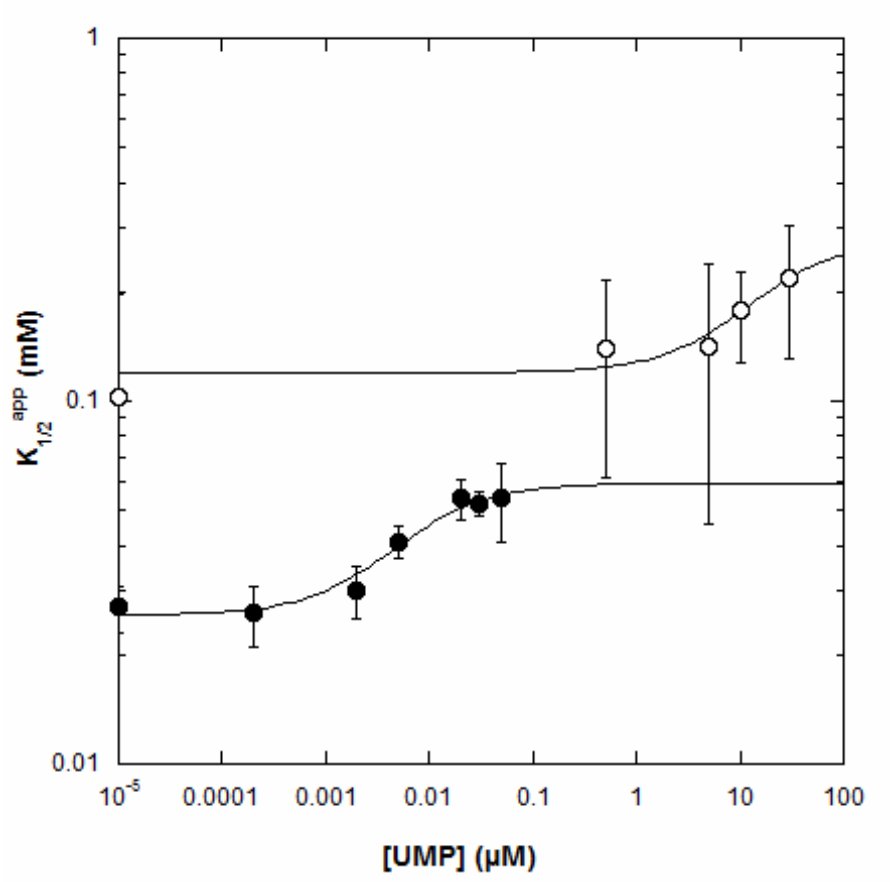

Figure 23: Plot of $K_{1/2}^{app}$ vs. UMP demonstrating allosteric inhibition of MgATP binding to the bicarbonate dependent ATPase site in both enzyme species, heterodimeric CPS in closed circles and large subunit of CPS in open circles at 25°C.

Enzyme Species	K_{ia}^{0}**(mM)**	K_{iy}^{0} **(mM)**	Q_{ay}
Heterodimer	0.026 ± 0.003	0.003 ± 0.002	0.43 ±0.07
Large subunit	0.12 ± 0.06	Undetermined	0.4 ± 0.5

Table 4: Thermodynamic dissociation constants extracted from data in Figure 23 according to Equation 3**.**

Following the same analysis method as Chapter IV, values of Q_{ay} were determined at various temperatures for each of the enzyme species. Figure 24 contains the data sets from experiments determining Q_{ay} at varying temperatures with fits to Equation 3. The data for the heterodimeric CPS (Top panel Figure 24) is well described by Equation 3 and shows inhibition at all temperatures, as indicated by the transition from a high affinity to lower affinity as UMP is added. Alternatively, the data in the bottom panel of Figure 24 represent the large subunit response to UMP at various temperatures. As is evident the distance between the lower and upper plateaus diminishes as temperature is increased and even becomes inverted when the temperature is raised to 30°C. The data were fit to Equation 3 to extract values for Q_{ay} which were then plotted for Van't Hoff analysis in Figure 25.

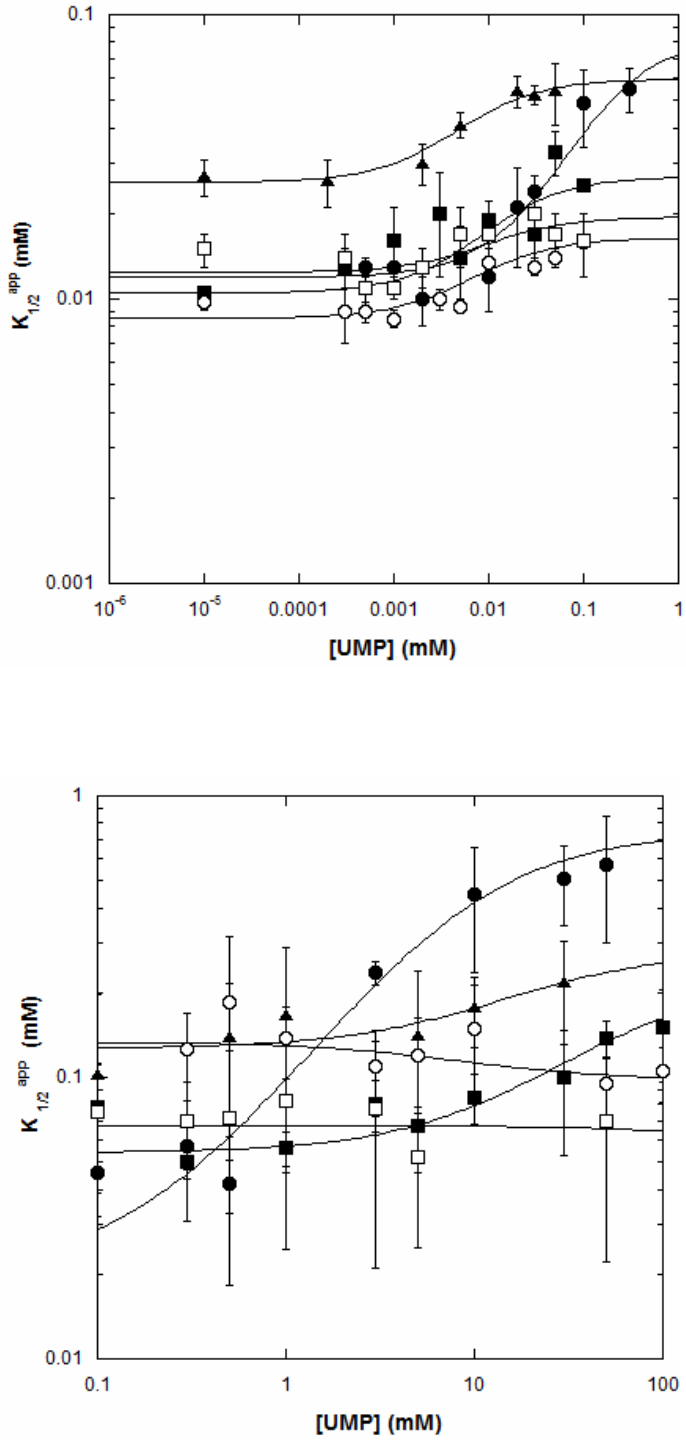

Figure 24: $K_{1/2}$ as a function of UMP concentration at varied temperatures for the bicarbonate dependent ATPase reaction of CPS. Top panel represents heterodimer data; bottom panel displays large subunit data. (●- 288K, ■- 293K, ♦- 298K, ○- 303K, □- 308K)

Inspection of the Van't Hoff plot suggests a significant change in the response of the allosteric effect with respect to temperature when the glutaminase subunit is removed. The values in

Table 5 represent the enthalpic and entropic components of the coupling free energy at 25°C, one can observe at this temperature the magnitude of the allosteric effect is similar in both enzyme species. However, due a stronger dependence on temperature the response of the large subunit to UMP exhibits a crossover point where the effect of UMP is expected to become activating. This crossover temperature is approximately 30°C.

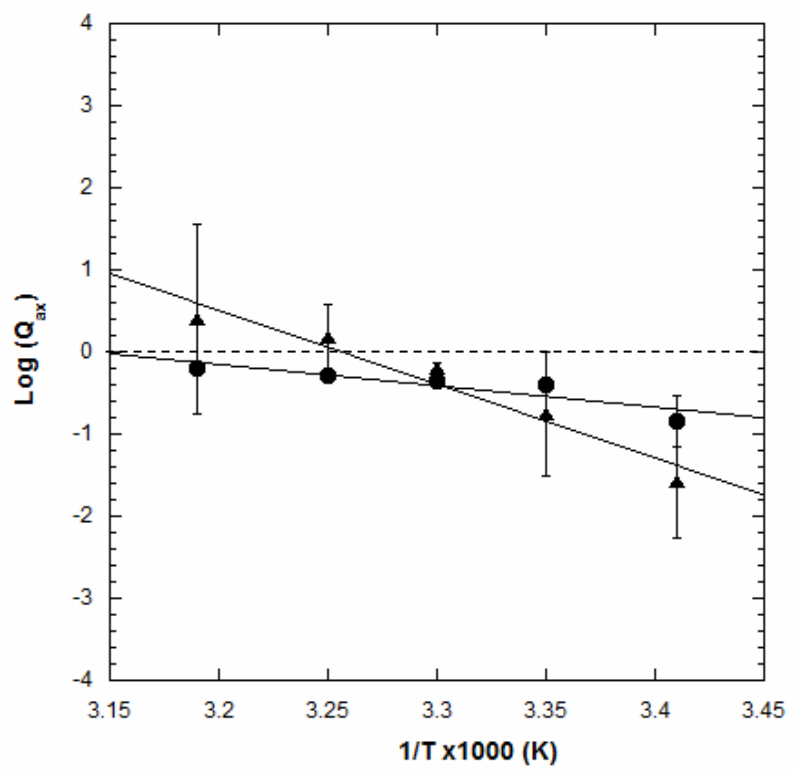

Figure 25: Van't Hoff plot for the allosteric response of the bicarbonate dependent ATPase activity of heterodimeric CPS (closed circles) and the large subunit of CPS in isolation (closed triangles).

Enzyme Species	**ΔH_{ay} (cal/mol)**	**$T\Delta S_{ay}$ (kcal/mol)**	**ΔG_{ay} (kcal/mol)**
Heterodimer	2 ± 0.6	-0.56 ± 0.02	0.56 ± 0.02
Large Subunit	9 ± 1	-1.0 ± 0.04	1.0 ± 0.04

Table 5: Thermodynamic parameters extracted from Van't Hoff analysis of the bicarbonate dependent ATPase reaction at 25°C.

ATP Synthesis Reaction

ATP synthesis is the reverse reaction of the final catalytic center in CPS. The third catalytic center is used to produce carbamoyl phosphate in the forward direction, illustrated in reaction 5. The inhibitory effect of UMP on the ATP synthesis reaction in heterodimeric CPS has been demonstrated by several researchers[20,39,84]. For completeness, the same systematic approach described in the Chapter IV was undertaken with the ATP synthesis reaction and the inhibitor UMP. In experiments performed with the heterodimeric CPS the concentration of carbamoyl phosphate was limited $\sim\frac{1}{3}K_m$ of CP so that the $K_{1/2}^{app}$ derived from the initial velocity studies approximates the thermodynamic dissociation constant K_{ia}^{0}.

As demonstrated in the Chapter IV, the catalytic activity of the ATP synthesis reaction is preserved when the subunit interface is liberated. These data represent the investigation of the allosteric effect of UMP on the ATP synthesis reaction when CPS is expressed and purified without the glutaminase subunit of the heterodimer.
The responsiveness of heterodimeric CPS to UMP was confirmed as before by Johnson et al[39]. Heterodimeric CPS exhibits a robust response to UMP at 25°C (Figure 26). As expected there is a shift in $K_{1/2}^{app}$ to the right indicates inhibition of binding substrate, MgADP. Unlike previous experiments with the activator, ornithine, there is a pronounced effect on the apparent V_m when UMP is at saturating concentrations. This effect has been reported previously and is as expected[20,39].

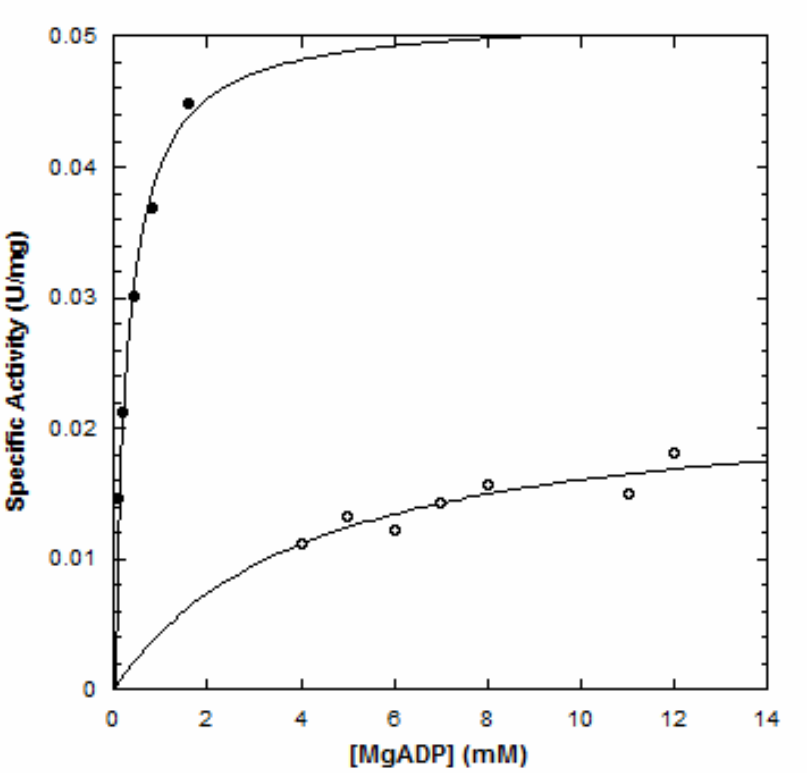

Figure 26: Specific activity of the ATP synthesis reaction of heterodimeric CPS vs MgADP at 25°C in the absence (closed circles) and saturating presence (10 mM) of UMP. Carbamoyl phosphate concentration 0.5 mM such that $\boldsymbol{K_{1/2}^{app}}$ approximates $\boldsymbol{K_{ia}}$.

.

Calculation of Q_{ay} from the $K_{1/2}^{app}$ for MgADP determined in the absence and saturating presence of UMP is performed under the following assumption: The limiting of CP concentration to ~ $\frac{1}{3}K_m$ generates a condition such that $K_{1/2}^{app}$ for MgADP approximates K_{ia}. Using thermodynamic linkage analysis principles, the argument has been made[34,35] that one can determine Q_{ay} from K_{ia}^{0} and K_{ia}^{∞}, the thermodynamic dissociation constant for substrate in the absence and saturating presence of UMP respectively, from the relationship described in Equation 4.

(4) $$Q_{ay} = \frac{K_{ia}^{0}}{K_{ia}^{\infty}} = \frac{K_{iy}^{0}}{K_{iy}^{\infty}}$$

Van't Hoff analysis of Q_{ay} demonstrates a modest dependence of Q_{ay} on temperature. The entropic and enthalpic components of the coupling free energy can be calculated from the best linear fit to the data in Figure 27 and are enumerated in Table 6 and are within error of those reported by Braxton *et al* in 1996[56].

The large subunit in isolation however, demonstrated no response to UMP in the ATP synthesis reaction. Initial experiments were performed using the previously described conditions of limited CP concentration and varied concentrations of MgADP to determine the K_{ia}^{0} and K_{ia}^{∞} (data not shown). Upon addition of up to 50 mM UMP no change in $K_{1/2}^{app}$ nor V_m was apparent.

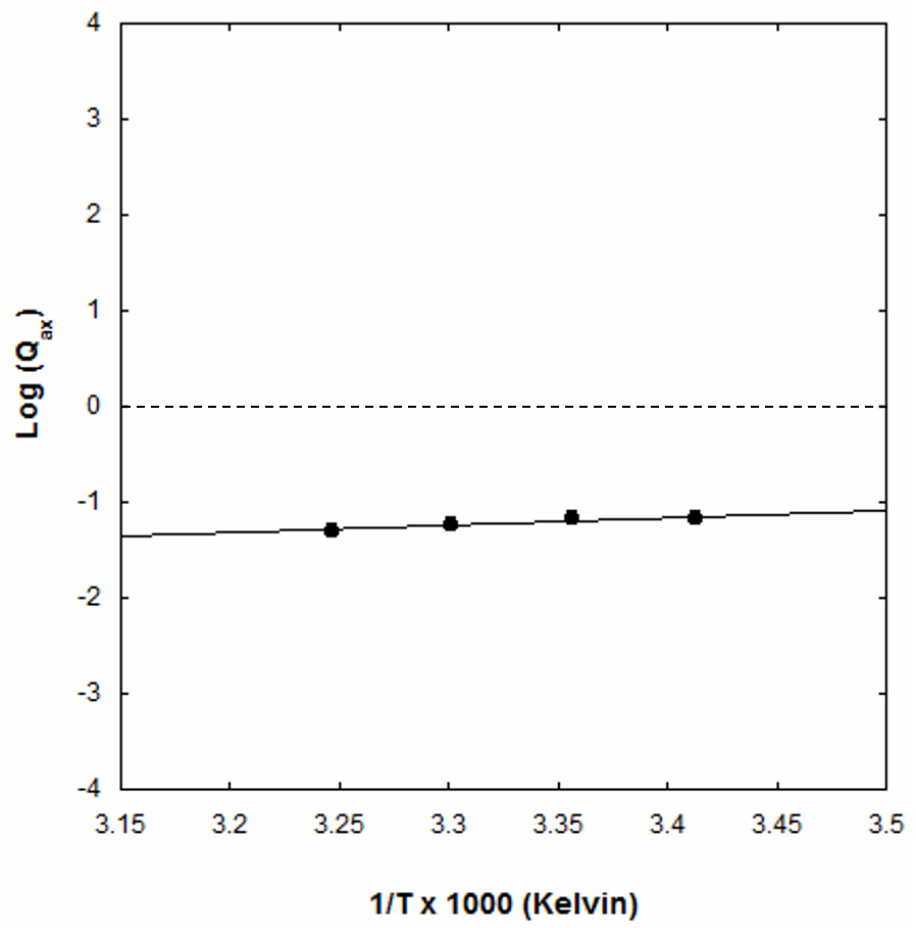

Figure 27: Van't Hoff analysis of the coupling between MgADP and UMP with respect to the ATP synthesis reaction of CPS. Plot is the logarithm of the coupling parameter $\boldsymbol{Q_{ax}}$ as a function of inverse temperature in Kelvin. Closed circles represent the data from heterodimer experiments. When not visible, error bars are smaller than symbols.

Enzyme Form	ΔH_{ay} **(cal/mol)**	ΔTS_{ay} **(kcal/mol)**	ΔG_{ay} **(kcal/mol)**
Heterodimer	-0.7 ± 0.02	-1 .6 ± 0.2	1.6 ± 0.2

Table 6: Thermodynamic components of the Gibb's free energy associated with the allosteric inhibition of MgADP binding by UMP in heterodimeric CPS extracted from the linear fit of the data in Figure 27.

In order to confirm the lack of response was not due to the system not satisfying the assumptions necessary for $K_{1/2}^{app}$ to approximate K_{ia} bi-substrate experiments were performed as in Chapter III of this dissertation. In addition to the previous methodology for direct determination of kinetic mechanism, here the parameters were determined in the presence of UMP at various concentrations to confirm the lack of response to UMP with regard to K_{ia}, K_a , K_b and V_m at 25°C (Figure 28). These data reinforce the conclusion from previous experiments that the large subunit of CPS in isolation exhibits no saturable allosteric response to UMP in any parameter measured in these experiments for the ATP synthesis reaction.

The lack of response at 25°C by the large subunit of CPS in the ATP synthesis reaction while surprising does not preclude the possibility that a response could occur at higher or lower temperatures. As such, the same experiments were conducted at 35°C (Figure 29) and 15°C (Figure 30). At both additional temperatures, all parameters demonstrate no dependence on the concentration of UMP in the assay supporting the conclusion that not only is the large subunit in isolation unresponsive to UMP with respect to the ATP synthesis reaction but, also there is no response to UMP at high or low temperature.

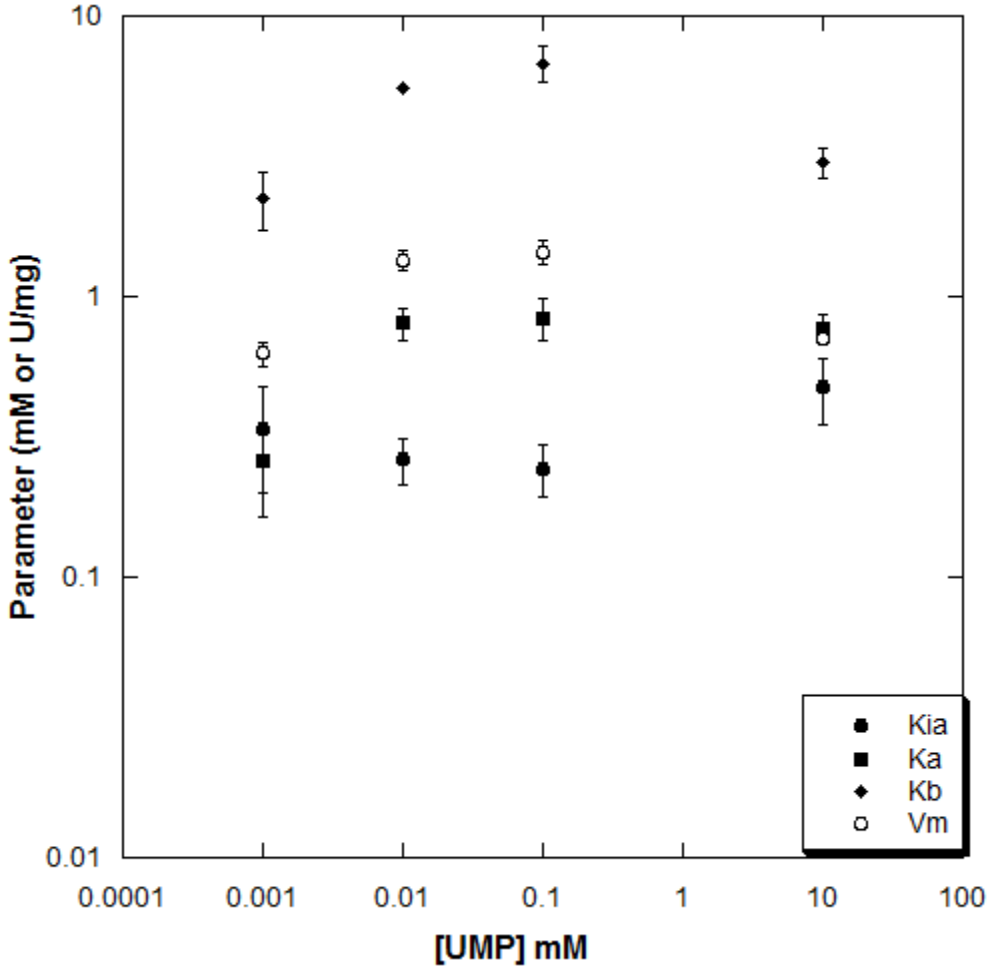

Figure 28: Plot of parameters from bisubstrate analysis of the ATP synthesis reaction of the large subunit of CPS in isolation 298K. The values plotted as a function of UMP were determined using the methods in Chapter III with the addition of a fixed concentration of UMP.

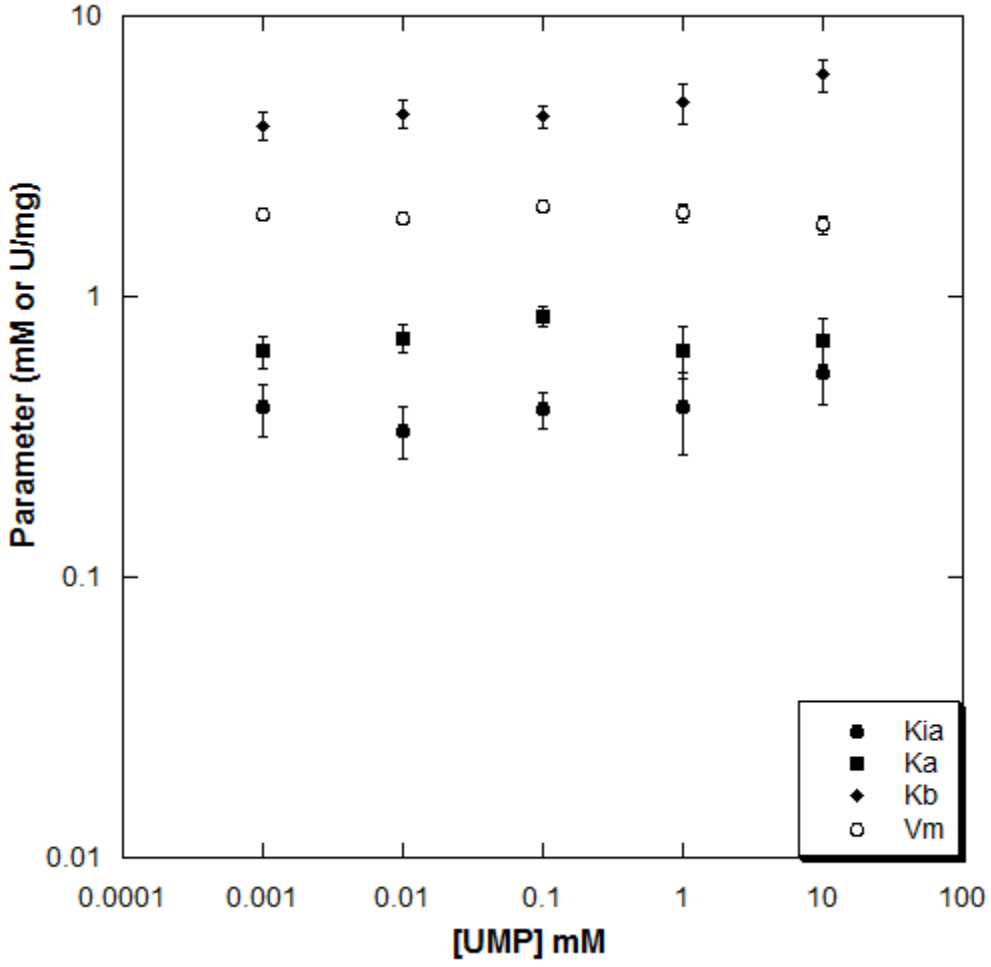

Figure 29: Plot of parameters from bisubstrate analysis of the ATP synthesis reaction of the large subunit of CPS in isolation 308K. The values plotted as a function of UMP were determined using the methods in Chapter III with the addition of a fixed concentration of UMP.

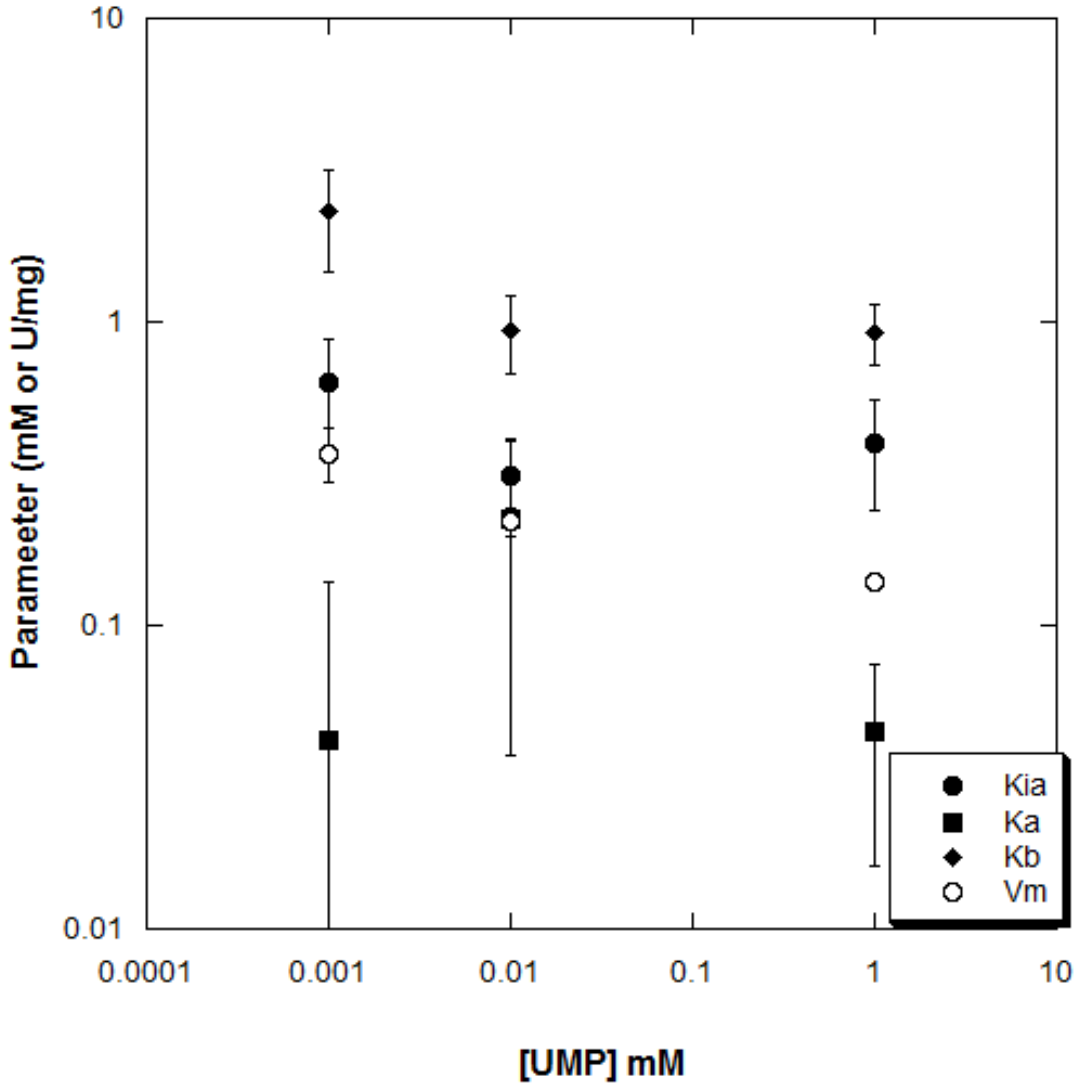

Figure 30: Plot of parameters from bisubstrate analysis of the ATP synthesis reaction of the large subunit of CPS in isolation 288K. The values plotted as a function of UMP were determined using the methods in Chapter III with the addition of a fixed concentration of UMP.

Discussion

The investigation of the entropy-enthalpy compensation of the coupling free energy between UMP and the ligands MgATP (bicarbonate dependent ATPase reaction) and MgADP (ATP synthesis reaction) in CPS provide an interesting story. Previous work by Braxton et al[56] investigated the dependence of the coupling free energy, ΔG_{ay},in heterodimeric CPS with respect to the ATP synthesis reaction only. The data presented therein provided ground work for the data presented here. The liberation of the subunit interface of heterodimeric CPS resulted in stark differences when compared to the allosteric effects seen in the wild type heterodimeric CPS.

Investigation of the allosteric response to UMP at the bicarbonate dependent ATPase reaction center did not demonstrate significant perturbation in the inhibition of MgATP binding (Figure 23) when the glutaminase subunit was removed. The measure of allosteric response, Q_{ay}, suggests that both the large subunit in isolation and the heterodimer have a value of approximately 0.4. In contrast, the dissociation constant for UMP, K_{iy}^{0}, is increased in the large subunit by three orders of magnitude. These changes are manifest while the dissociation constant for MgATP, K_{ia}^{0}, is perturbed on much more modest scale, showing an increase from 26 μM to 120 μM with and without the glutaminase subunit, respectively.

The changes in parameters observed are quite interesting as the bicarbonate dependent ATPase reaction center is directly proximal to the subunit interface. One would suppose the K_{ia}^{0} for MgATP would be affected more dramatically than the K_{iy}^{0} as

the binding site for substrate is 45 Å closer to the subunit interface than the binding site for UMP.

Van't Hoff analysis of Q_{ay} at 298K reveals that the allosteric inhibition engendered by UMP is entropically driven in both enzyme species. The enthalpy component of ΔG_{ay} for both heterodimer and large subunit are small in absolute terms, 2 cal/mol ±0.6 and 9 cal/mol ± 1 respectively, compared to the entropy component -0.56 kcal/mol ± 0.02 and -1.0 ± 0.04 kcal/mol, as before. Also, evident from this analysis is the origin of the increased inhibition by UMP. The entropy component is dominant in the interaction and the large subunit in isolation exhibits larger unfavorable entropy than the heterodimer. As the enthalpic component in both enzyme species is negligible the increase in ΔG_{ay} and consequently, the increased inhibition by UMP is due to the increase in the absolute value of the $T\Delta S_{ay}$ term.

With respect to UMP inhibition it appears that the liberation of the subunit interface has resulted in a larger absolute value of $T\Delta S_{ay}$ in the large subunit over that demonstrated by the heterodimer. The increase in $T\Delta S_{ay}$ should not be confused with the increase in entropy associated with the liberation of the subunit interface. $T\Delta S_{ay}$ is the entropy component of the coupling free energy, the free energy associated with the allosteric response.

Of particular interest is the observation of a crossover point in the allosteric response of the bicarbonate dependent ATPase. At approximately 25°C the Van't Hoff plot crosses zero indicating that $Log(Q_{ay}) = 0$ and by extension $\Delta G_{ay} = 0$.

Temperatures above this crossover point lead to activation while temperatures lower engender an inhibitory effect.

The crossover point evident here is not the first example of the phenomenon, in fact the third allosteric ligand for CPS, inosine monophosphate (IMP), exhibits a crossover point at 37°C when IMP affects are investigated in the ATP synthesis reaction of the heterodimer[55]. PFK from *Bacillus stearothermophilus* also demonstrates a crossover point related to its effector ADP at approximately 16°C[55].

When the ATP synthesis reaction is considered, data presented here are in agreement with that published by Braxton et al[20]. The heterodimer of CPS exhibits inhibition by UMP increasing the K_{ia} from 0.28 mM ± 0.03 in the absence of UMP to 4.1 mM ± 1.4 in the saturating presence of UMP (10 mM). The temperature dependence of Q_{ay} also agrees with previously published data[56]. The Van't Hoff analysis of the heterodimer response to UMP reveals ΔG_{ay}= 1.6 kcal/mol ± 0.2. The entropic component, $T\Delta S_{ay}$, is -1.6 kcal/mol ± 0.2 and its absolute value is larger than the enthalpic component,ΔH_{ay} = -0.7 cal/mol ± 0.2 representing the entropy dominant nature of inhibition by UMP in CPS.

However, when the large subunit of CPS is interrogated in isolation from the glutaminase subunit the allosteric response to UMP is abolished in the ATP synthesis reaction. Bi-substrate analysis of the ATP synthesis reaction allowed determination of K_{ia}, K_a , K_b and V_m at varying concentrations of UMP and temperature to confirm the loss of allosteric response to UMP. At 25°C all four parameters exhibit no change

with UMP concentration up to 10 mM. When the temperature was raised to 35°C parameters again remained constant up to 10 mM UMP.

The loss of allosteric inhibition by UMP of the ATP synthesis reaction is unexpected as the subunit interface is approximately 45Å removed from the reaction center while the binding site of UMP is directly adjacent to the reaction center. This suggests that the allosteric communication for UMP inhibiting the binding of MgADP necessitates the presence of the glutaminase subunit. When the loss of inhibition in the ATP synthesis reaction is considered in tandem with the enhancement of inhibition in the bicarbonate dependent ATPase reaction the results suggest that UMP has two different conduits of action to inhibit the partial reactions of CPS.

One proposed communication pathway for the inhibition of the ATP synthesis reaction is that the pathway for transmission for the allosteric signal is broken upon the liberation of the interface, either by removing part of the conduit that extends into the glutaminase subunit or, disrupting the connectivity via loosened conformational constraints in regions near the interface.

The results from the bicarbonate dependent ATPase reaction suggest the possibility of a second conduit of communication between the allosteric site and active site which was not disturbed by the liberation of the subunit interface. However, one cannot rule out the possibility of yet another mode of allosteric communication. It is possible that there is no network of interactions along a specific pathway but, a global rigidification or loosening of side chains that result in the allosteric response. While posing a different method of action, the same logic can be applied as before resulting in

the necessity for two distinct networks to communicate the inhibitory signal to the individual reaction centers on the large subunit of CPS.

CHAPTER VI

SUMMARY

The reactions catalyzed by the large subunit of CPS demonstrate intriguing differences when interrogated in the presence and absence of the smaller, glutaminase subunit. As demonstrated the bicarbonate dependent ATPase reaction and the ATP synthesis reaction are both viable upon removal of the glutaminase subunit. This, however, has been previously demonstrated[87]. Interestingly, the investigation into the mechanism of the ATP synthesis reaction with the large subunit in isolation presented distinct differences when compared to the same reaction with the heterodimer.

The ATP synthesis reaction of CPS demonstrated significant response to the liberation of the subunit interface. From the bi-substrate analysis presented in Chapter III of this work one can see that the Michaelis constant for MgADP is increased by more than 25-fold from 16 μM to 420 μM. Also, demonstrating a significant increase is the Michaelis constant for CP. The K_b increased 3.5-fold from 0.66 mM to 2.4 mM. Interestingly, the dissociation constant for MgADP was not significantly affected by the liberation of the subunit interface. The K_{ia} values determined were 200 ±30 μM and 250 ±80 μM in the heterodimer and the large subunit in isolation, respectively. Another parameter of comparison is the turnover numbers of each enzyme species. The heterodimeric CPS exhibits a k_{cat} of 0.266±0.008 sec^{-1} while the large subunit in isolation demonstrates a k_{cat} of 0.06±0.01 sec^{-1}.

Most striking is the dramatic shifts in the patterns of the primary plots of reciprocal specific activity versus reciprocal substrate. These plots, Figure 9 for the heterodimer and Figure 11 for the large subunit, demonstrate the profound effect removing the glutaminase subunit engendered on the ATP synthesis reaction. The secondary plots, Figure 10 and Figure 12 also demonstrate shifts in the y-axis intercepts further indicating that the kinetic mechanism has been perturbed in some way.

The reciprocal plots for the ATP synthesis reaction with the heterodimer indicate a sequential mechanism. The secondary plots presented in this work do not offer any further insight to the mechanism. This is in contrast to the work published by Braxton et al[20]. Braxton reported that the secondary plot of the bi-substrate analysis with CP held constant results in the slope extrapolating through the origin. Braxton's data suggests that the ATP synthesis reaction proceeds through an equilibrium ordered mechanism. The discrepancy while present, does not have significant impact on the results presented here. The shifts seen in the plots with the large subunit in isolation compared to those of the heterodimer clearly demonstrate a perturbation to the kinetic mechanism while remaining sequential in nature.

The allosteric effect of ornithine presented in Chapter IV demonstrates contrasting effects on the two interrogated reaction centers. The effect of ornithine on the bicarbonate dependent ATPase reaction is enhanced upon removal of the glutaminase subunit while the response to ornithine in the ATP synthesis is attenuated.

The increase in allosteric response to ornithine in the bicarbonate dependent ATPase reaction is reflected in the 1.1 kcal/mol further decrease in an already negative

ΔG_{ax}. The decrease in ΔG_{ax} can be attributed to the increase in the $T\Delta S_{ax}$ term even though there is also a very modest decrease in ΔH_{ax} as well. The favorable increase in the entropy term compensates for the decrease in the enthalpy term.

Contrarily, when investigating the ornithine effect on the ATP synthesis reaction the removal of the glutaminase subunit results in attenuation of the activation. The ΔG_{ax} is 0.8 kcal/mol less negative when compared to the heterodimer. The increase in ΔG_{ax} is indicative of a less favorable interaction between the substrate, MgADP, and the effector ornithine. With regard to the thermodynamic components of the interaction, the ΔH_{ax} component is negligible resulting in the change in $T\Delta S_{ax}$ dominating the enthalpy-entropy compensation.

Of particular note is the proximity of the two reaction centers and the impact of the liberation of the subunit interface. As expected, with the bicarbonate dependent ATPase reaction center being closer to the liberated interface, the increase in the configurational freedom had a more significant impact on the bicarbonate dependent ATPase reaction than the ATP synthesis reaction. Surprisingly, the ATP synthesis reaction demonstrated a decrease of 0.8 kcal/mol in the entropic component when the glutaminase subunit was absent. The decrease in $T\Delta S_{ax}$ is plausible since $T\Delta S_{ax}$ is not a measure of the entropy of the system resulting from the liberation of the subunit interface but, a comparison between the $T\Delta S_{ax}$ associated with the disproportionation equilibrium of the four possible ligated states of the enzyme.

Inhibition by UMP presents yet another interesting insight into the allosteric network at work in CPS. UMP binds at a site distinct from ornithine[66,89]. The work

presented in Chapter V demonstrates an intriguing effect caused by the removal of the glutaminase subunit. The allosteric response of the bicarbonate dependent ATPase reaction is preserved even if the binding of UMP is worse by 3 orders of magnitude. However, the allosteric inhibition of the ATP synthesis reaction appears to be abolished when the small subunit is removed.

The bicarbonate dependent ATPase reaction of heterodimeric CPS binds UMP with a dissociation constant of 3 μM while the large subunit in isolation demonstrates a dissociation constant for UMP of 8 mM. These data are a good example of the fact that binding and strength of allosteric effect are not linked, as the value of Q_{ay} for both enzyme species is approximately 0.4 despite the massive difference in dissociation constant for UMP. The discontinuity between binding and allosteric effect has been demonstrated previously. McGresham and Reinhart demonstrated the binding of PEP to *Thermus thermophilus* PFK is very tight while engendering only a modest allosteric inhibition when compared to PFK from *Bacillus steareothermophilus* which binds PEP with a lower affinity and exhibits a robust allosteric inhibition[33].

Another fascinating phenomenon suggested by the Van't Hoff analysis of the bicarbonate dependent ATPase reaction dependence on UMP is the existence of a crossover point in the data for the large subunit in isolation. The crossover point in a Van't Hoff plot of Q_{ay} is when the trendline crosses the x-axis and indicates an inversion in the allosteric effect by the corresponding ligand. In Chapter V the data in Figure 25 indicate that the crossover point occurs at approximately 30°C. This is not the first time that a crossover has been see in allosteric enzymes. In 1989 Reinhart et al

published data for isocitrate dehydrogenase that demonstrated a theoretical crossover point that was experimentally unattainable[57]. In that publication, the authors set up the implications and reasoning behind the allosteric inversion. Then in 1994, Braxton et al. demonstrated that the allosteric effector of CPS, IMP, exhibits a crossover point an experimentally attainable temperature range[55]. Considering there is a foundation of work establishing these crossover points as significant[55,57] and the added fact that CPS has two ligands, IMP and UMP, that exhibit crossover, the further investigation of the entropic component of the allosteric effect is of great interest.

The response of the ATP synthesis reaction to UMP raises questions as well. The heterodimeric CPS responded as expected, 1.6 kcal/mol for ΔG_{ay}. The question arises when the large subunit is interrogated in isolation. The large subunit demonstrates no saturable allosteric effect from UMP. The bi-substrate analysis performed in Chapter III and Chapter V report on several kinetic and a thermodynamic parameter for the reaction, K_{ia}, K_a, K_b, V_{max}. Upon interrogation of the effect UMP has on the large subunit of CPS using the bi-substrate analysis there were no discernable trends that would describe an allosteric interaction. As is evident form Figure 28 and Figure 30 there are effects on the monitored parameters which suggests UMP is binding. Confidence in UMP binding to the large subunit is high as the bicarbonate dependent ATPase reaction is responsive to UMP.

Ornithine and UMP both regulate heterodimeric CPS bicarbonate dependent ATPase and ATP synthesis however, the large subunit in isolation exhibits changes in the regulation of each reaction with respect to each ligand. If one considers that ornithine

and UMP bind to sites distinct from one another on CPS[90,91] then it is reasonable that the pathways of allosteric communication of the two ligands could be different.

According to data in Figure 15 at 25°C the removal of the large subunit causes a 5-fold increase of the allosteric effect of ornithine on the bicarbonate dependent ATPase reaction. This suggests that the communication between the ornithine binding site and the bicarbonate dependent ATPase reaction center is preserved upon removal of the glutaminase subunit even though there is approximately 39 Å distance between the sites.

The ATP synthesis site is directly proximal to the ornithine binding site and a hydrogen bonding network was suggested as a possible connection between the two sites[91]. Interestingly, the data in Figure 18 shows that the removal of the small subunit results in a severe reduction in allosteric activation by ornithine. The significant impact on Q_{ax} is in contradiction to expectation as the perturbation is almost 45 Å distal to both the ornithine binding site and the ATP synthesis reaction center. The seemingly discontinuous result further reinforces the ideas that allosteric communication can be more complicated than a direct pathway between sites and that the $T\Delta S_{ax}$ parameter is not a measure of the systemic entropy of the enzyme but the entropic component of the interaction between ornithine and MgADP. In this instance while general entropy is increased by the liberation of the subunit interface, the $T\Delta S_{ax}$ is actually decreased.

The inhibition of the two enzyme species by UMP also demonstrates evidence for a complex mode of allosteric communication. The bicarbonate dependent ATPase reaction is sensitive to UMP in both constructs while the ATP synthesis reaction is only sensitive to UMP binding in the heterodimer.

The bicarbonate dependent ATPase reaction of CPS demonstrates no appreciable difference in the magnitude of the allosteric inhibition by UMP upon removal of the glutaminase subunit. However, there is a significant shift, 4 orders of magnitude, in the affinity for MgATP. The thermodynamic components of the UMP inhibition are both increased upon removal of the glutaminase subunit as well. ΔH_{ay} is increased by 0.007 kcal/mol while $T\Delta S_{ay}$ is increased by 0.5 kcal/mol. Similar to the ornithine activation this impact is observed at the reaction center that is closest to the subunit interface yet removed from the allosteric binding site by 39 Å.

The ATP synthesis reaction response to UMP is indicative of a unique allosteric communication between the binding sites for MgADP and UMP. In the heterodimer the inhibition of the ATP synthesis reaction behaves as reported in the literature[20,31]. The large subunit however demonstrates no saturable allosteric response in K_{ia}, K_a, K_b, nor V_{max} at any temperature investigated (Figures 28-30). These data suggest that the allosteric communication between UMP and the MgADP of the ATP synthesis reaction is disrupted upon the removal of the glutaminase subunit. The lack of allosteric communication between UMP and MgADP was unexpected as the ATP synthesis reaction center is only about 10 Å away from the binding site for UMP leading to the expectation of a localized communication network.

While the work presented here characterizes the large subunit of CPS in detail not previously explored there are several thoughts that stem from findings. These thoughts present solid platforms for further investigation.

Of particular interest is further investigation of the crossover point generated in the UMP response of the bicarbonate dependent ATPase reaction when the large subunit is interrogated in isolation. It would be interesting to perform a Van't Hoff analysis on the impact of IMP on the bicarbonate dependent ATPase reaction to determine if there is a physiologically relevant crossover point in that allosteric interaction as well. The interaction could then be investigated above and below the crossover point to interrogate residues involved in activation versus inhibition.

The most intriguing continuation of this research would be to investigate the motion of secondary structural elements of the large subunit compared to that in the heterodimer. As the allosteric effects reported here heavily favor the entropic component of the coupling free energy it would be of great interest to see if the anisotropy of particular regions of CPS show change upon the loss of the small subunit. A mutant of the heterodimer has already been made in which the 6 native tryptophan have been mutated to tyrosine[39]. This construct would allow for the use of intrinsic tryptophan fluorescence to measure anisotropy and report on local movements upon ligand binding.

Another question raised by this research pertains to the mechanism of the ATP synthesis reaction. The data suggests that the reaction is sequential but, more experiments are needed to determine fully the order of addition of substrates.

The removal of the glutaminase subunit causes a significant shift in the diagnostic double reciprocal plots for determination of the kinetic mechanism of the ATP synthesis reaction.

Also, liberating the subunit interface causes stark changes in the regulation of the reaction centers by ornithine. The loss of interfacial restraints causes ornithine activation to increase in the bicarbonate dependent ATPase reaction while causing a decrease in allosteric activation at the ATP synthesis site.

The magnitude of the allosteric effect of UMP at the bicarbonate dependent ATPase reaction is not significantly affected by removal of the small subunit. However, the data presented here suggest that inhibition by UMP at the ATP synthesis site is completely abolished when interfacial constraints are removed.

When considering the dramatic differences liberating the subunit interface has on the regulation of the active sites of CPS one must step back and ponder the implications the results have on the structure of the enzyme. The lack of severe perturbation to the kinetic mechanisms of the partial reactions suggest that there are no general changes to the fold and structure of the enzyme and the increased entropy components seen in the Van't Hoff analysis is due to a shift in the internal entropy of the four enzyme species found in the disproportionation equilibrium. However, Q_{ax} does not provide any insight into which of the four enzyme species experience the most entropic perturbations as a result of easing interfacial constraints. As a result, one can parse out the entropic component of the allosteric coupling free energy and still not be able to determine if increasing the entropic component will augment or attenuate the allosteric response by a particular ligand pair.

This research demonstrates the need for continuing research in allosteric regulation of enzymes, especially in the face of the emerging drug market for allosteric

ligands. The data presented here indicates that a cursory knowledge of the mode of allosteric regulation, in this case the entropy dominated nature, does not reflect a complete understanding of the interaction. The research suggests that interrogating potential drugs through linkage analysis and possibly even Van't Hoff analysis of the coupling quotient will provide a better picture of the coupling between a potential allosteric drug, its target enzyme and that enzyme's active site ligand. A better understanding of the free energy and the corresponding enthalpy-entropy compensation will allow further refinement of targeting and effect of future allosteric drugs.

In conclusion, the research presented here demonstrates that there is significant impact on the partial reactions of CPS located on the large subunit upon liberation of the subunit interface. There are also significant perturbations to the allosteric effects of ornithine and UMP on both reaction centers.

REFERENCES

(1) Monod, J., Wyman, J., and Changeux, J. P. (1965) on the Nature of Allosteric Transitions: a Plausible Model. *J. Mol. Biol. 12*, 88–118.

(2) Pauling, L. (1935) The Oxygen Equilibrium of Hemoglobin and Its Structural Interpretation. *Proc. Natl. Acad. Sci. U. S. A. 21*, 186–91.

(3) Perutz, M. F., Wilkinson, A. J., Paoli, M., and Dodson, G. G. (1998) The stereochemical mechanism of the cooperative effects in hemoglobin revisited. *Annu Rev Biophys Biomol Struct 27*, 1–34.

(4) Gill, S. J., Di Cera, E., Doyle, M. L., and Robert, C. H. (1988) New twists on an old story: hemoglobin. *Trends Biochem Sci 13*, 465–467.

(5) Warburg, O. (1956) On the Origin of Cancer Cells. *Science (80-.). 123*, 309–314.

(6) Blangy, D., Buc, H., and Monod, J. (1968) Kinetics of the allosteric interactions of phosphofructokinase from Escherichia coli. *J Mol Biol 31*, 13–35.

(7) Tlapak-Simmons, V. L., and Reinhart, G. D. (1994) Comparison of the inhibition by phospho(enol)pyruvate and phosphoglycolate of phosphofructokinase from B. stearothermophilus. *Arch Biochem Biophys 308*, 226–230.

(8) Johnson, J. L., and Reinhart, G. D. (1997) Failure of a two-state model to describe the influence of phospho(enol)pyruvate on phosphofructokinase from Escherichia coli. *Biochemistry 36*, 12814–12822.

(9) Johnson, J. L., and Reinhart, G. D. (1994) Influence of substrates and MgADP on the time-resolved intrinsic fluorescence of phosphofructokinase from Escherichia coli. Correlation of tryptophan dynamics to coupling entropy. *Biochemistry 33*, 2644–2650.

(10) Ortigosa, A. D., Kimmel, J. L., and Reinhart, G. D. (2004) Disentangling the web of allosteric communication in a homotetramer: heterotropic inhibition of phosphofructokinase from Bacillus stearothermophilus. *Biochemistry 43*, 577–586.

(11) Shirakihara, Y., and Evans, P. R. (1988) Crystal structure of the complex of phosphofructokinase from Escherichia coli with its reaction products. *J Mol Biol 204*, 973–994.

(12) Shirakiharat, Y., and Evans, P. R. (1988) Crystal Structure of the Complex of Phosphofructokinase from Escherichia coli With its Reaction Products. *J. Mol. Biol 204*, 973–994.

(13) Feliú, J. E., Hue, L., and Hers, H. G. (1976) Hormonal control of pyruvate kinase activity and of gluconeogenesis in isolated hepatocytes. *Proc Natl Acad Sci U S A 73*, 2762–2766.

(14) van Veelen, C. W., Verbiest, H., Zülch, K. J., van Ketel, B. A., van der Vlist, M. J., Vlug, A. M., Rijksen, G., and Staal, G. E. (1979) L-alpha-alanine inhibition of pyruvate kinase from tumors of the human central nervous system. *Cancer Res 39*, 4263–4269.

(15) Valentini, G., Chiarelli, L., Fortin, R., Speranza, M. L., Galizzi, A., and Mattevi, A. (2000) The allosteric regulation of pyruvate kinase. *J Biol Chem 275*, 18145–18152.

(16) Mattevi, A., Bolognesi, M., and Valentini, G. (1996) The allosteric regulation of pyruvate kinase. *FEBS Lett 389*, 15–19.

(17) Hall, E. R., and Larry Cottam, G. (1978) Isozymes of pyruvate kinase in vertebrates: their physical, chemical, kinetic and immunological properties. *Int. J. Biochem. 9*, 785–794.

(18) Jurica, M. S., Mesecar, A., Heath, P. J., Shi, W., Nowak, T., and Stoddard, B. L. (1998) The allosteric regulation of pyruvate kinase by fructose-1,6-bisphosphate. *Structure 6*, 195–210.

(19) Rodríguez, M., Good, T. A., Wales, M. E., Hua, J. P., and Wild, J. R. (2005) Modeling allosteric regulation of de novo pyrimidine biosynthesis in Escherichia coli. *J. Theor. Biol. 234*, 299–310.

(20) Braxton, B. L., Mullins, L. S., Raushel, F. M., and Reinhart, G. D. (1992) Quantifying the allosteric properties of Escherichia coli carbamyl phosphate synthetase: determination of thermodynamic linked-function parameters in an ordered kinetic mechanism. *Biochemistry 31*, 2309–2316.

(21) Duggan, K. C., Walters, M. J., Musee, J., Harp, J. M., Kiefer, J. R., Oates, J. A., Marnett, L. J., and Hancock, A. B. (2010) Molecular Basis for Cyclooxygenase Inhibition by the Non-steroidal Anti-inflammatory Drug Naproxen * □ S. *Publ. JBC Pap. Press*.

(22) Crofford, L. J. (1997) COX-1 and COX-2 tissue expression: implications and predictions. *J. Rheumatol. Suppl. 49*, 15–9.

(23) Chavez, M. L., and DeKorte, C. J. (2003) Valdecoxib: A review. *Clin. Ther. 25*, 817–851.

(24) Busson, M. (1986) Update on Ibuprofen: Review Article. *J Int Med Res 14*.

(25) Kurumbail, R. G., Stevens, A. M., Gierse, J. K., McDonald, J. J., Stegeman, R. A., Pak, J. Y., Gildehaus, D., iyashiro, J. M., Penning, T. D., Seibert, K., Isakson, P. C., and Stallings, W. C. (1996) Structural basis for selective inhibition of cyclooxygenase-2 by anti-inflammatory agents. *Nature 384*, 644–648.

(26) Vane, J. R., and Botting, R. M. The mechanism of action of aspirin.

(27) Husted, S., and van Giezen, J. J. J. (2009) Ticagrelor: the first reversibly binding oral P2Y12 receptor antagonist. *Cardiovasc. Ther. 27*, 259–74.

(28) Cattaneo, M. (2010) New P2Y12 Inhibitors. *Circulation 121*.

(29) VAN GIEZEN, J. J. J., NILSSON, L., BERNTSSON, P., WISSING, B.-M., GIORDANETTO, F., TOMLINSON, W., and GREASLEY, P. J. (2009) Ticagrelor binds to human P2Y $_{12}$ independently from ADP but antagonizes ADP-induced receptor signaling and platelet aggregation. *J. Thromb. Haemost. 7*, 1556–1565.

(30) Tlapak-Simmons, V. L., and Reinhart, G. D. (1994) Comparison of the inhibition by phospho(enol)pyruvate and phosphoglycolate of phosphofructokinase from B. stearothermophilus. *Arch Biochem Biophys 308*, 226–230.

(31) Braxton, B. L., Mullins, L. S., Raushel, F. M., and Reinhart, G. D. (1999) Allosteric dominance in carbamoyl phosphate synthetase. *Biochemistry 38*, 1394–1401.

(32) McGresham, M. S., Lovingshimer, M., and Reinhart, G. D. (2014) Allosteric regulation in phosphofructokinase from the extreme thermophile Thermus thermophilus. *Biochemistry 53*, 270–8.

(33) Mcgresham, M. S., and Reinhart, G. D. Enhancing Allosteric Inhibition in Thermus thermophilus Phosphofructokinase.

(34) Reinhart, G. D. (1983) The determination of thermodynamic allosteric parameters of an enzyme undergoing steady-state turnover. *Arch Biochem Biophys 224*, 389–401.

(35) Reinhart, G. D. (2004) Quantitative analysis and interpretation of allosteric behavior. *Methods Enzym. 380*, 187–203.

(36) Reinhart, G. D. (1980) Evaluation of first-order kinetic transients encountered during enzyme assay. *Anal Biochem 104*, 99–105.

(37) Bigley, A. N., and Reinhart, G. D. The N-terminus of glycogen phosphorylase B is not required for activation by adenosine 5'-monophosphate. *Biochemistry 49*, 4760–4765.

(38) Riley-Lovingshimer, M. R., and Reinhart, G. D. (2005) Examination of MgATP binding in a tryptophan-shift mutant of phosphofructokinase from Bacillus stearothermophilus. *Arch Biochem Biophys 436*, 178–186.

(39) Johnson, J. L., West, J. K., Nelson, A. D., and Reinhart, G. D. (2007) Resolving the fluorescence response of Escherichia coli carbamoyl phosphate synthetase: mapping intra- and intersubunit conformational changes. *Biochemistry 46*, 387–397.

(40) Symcox, M. M., and Reinhart, G. D. (1992) A steady-state kinetic method for the verification of the rapid-equilibrium assumption in allosteric enzymes. *Anal Biochem 206*, 394–399.

(41) Hydesg, C. C., Ahmedliii, S. A., Padlans, E. A., Milesli, E. W., and Daviess, D. R. (1988) Three-dimensional Structure of the Tryptophan Synthase *263*.

(42) Anderson, P. M., and Meister, A. (1966) Control of Escherichia coli carbamyl phosphate synthetase by purine and pyrimidine nucleotides. *Biochemistry 5*, 3164–3169.

(43) Trotta, P. P., Pinkus, L. M., Haschemeyer, R. H., and Meister, A. (1974) Reversible dissociation of the monomer of glutamine-dependent carbamyl phosphate synthetase into catalytically active heavy and light subunits. *J Biol Chem 249*, 492–499.

(44) Anderson, P. M., and Meister, A. (1966) Bicarbonate-dependent cleavage of adenosine triphosphate and other reactions catalyzed by Escherichia coli carbamyl phosphate synthetase. *Biochemistry 5*, 3157–3163.

(45) Thoden, J. B., Holden, H. M., Wesenberg, G., Raushel, F. M., and Rayment, I. (1997) Structure of carbamoyl phosphate synthetase: a journey of 96 A from substrate to product. *Biochemistry 36*, 6305–6316.

(46) Holden, H. M., Thoden, J. B., and Raushel, F. M. (1999) Carbamoyl phosphate synthetase: an amazing biochemical odyssey from substrate to product. *Cell Mol Life Sci 56*, 507–522.

(47) Nyunoya, H., and Lusty, C. J. (1983) The carB gene of Escherichia coli: a duplicated gene coding for the large subunit of carbamoyl-phosphate synthetase. *Proc Natl Acad Sci U S A 80*, 4629–4633.

(48) Thoden, J. B., Raushel, F. M., Benning, M. M., Rayment, I., and Holden, H. M. (1999) The structure of carbamoyl phosphate synthetase determined to 2.1 A resolution. *Acta Crystallogr D Biol Crystallogr 55*, 8–24.

(49) Thoden, J. B., Holden, H. M., Wesenberg, G., Raushel, F. M., and Rayment, I. (1997) Structure of carbamoyl phosphate synthetase: a journey of 96 A from substrate to product. *Biochemistry 36*, 6305–6316.

(50) Anderson, P. M. (1977) Binding of allosteric effectors to carbamyl-phosphate synthetase from Escherichia coli. *Biochemistry 16*, 587–593.

(51) Thoden, J. B., Huang, X., Kim, J., Raushel, F. M., and Holden, H. M. (2004) Long-range allosteric transitions in carbamoyl phosphate synthetase. *Protein Sci 13*, 2398–2405.

(52) Stapleton, M. A., Javid-Majd, F., Harmon, M. F., Hanks, B. A., Grahmann, J. L., Mullins, L. S., and Raushel, F. M. (1996) Role of conserved residues within the carboxy phosphate domain of carbamoyl phosphate synthetase. *Biochemistry 35*, 14352–14361.

(53) Czerwinski, R. M., Mareya, S. M., and Raushel, F. M. (1995) Regulatory changes in the control of carbamoyl phosphate synthetase induced by truncation and mutagenesis of the allosteric binding domain. *Biochemistry 34*, 13920–13927.

(54) Raushel, F. M., Mullins, L. S., and Gibson, G. E. (1998) A stringent test for the nucleotide switch mechanism of carbamoyl phosphate synthetase. *Biochemistry 37*, 10272–10278.

(55) Braxton, B. L., Tlapak-Simmons, V. L., and Reinhart, G. D. (1994) Temperature-induced inversion of allosteric phenomena. *J Biol Chem 269*, 47–50.

(56) Braxton, B. L., Mullins, L. S., Raushel, F. M., and Reinhart, G. D. (1996) Allosteric effects of carbamoyl phosphate synthetase from Escherichia coli are entropy-driven. *Biochemistry 35*, 11918–11924.

(57) Reinhart, G. D., Hartleip, S. B., and Symcox, M. M. (1989) Role of coupling entropy in establishing the nature and magnitude of allosteric response. *Proc Natl Acad Sci U S A 86*, 4032–4036.

(58) Trotta, P. P., Burt, M. E., Haschemeyer, R. H., and Meister, A. (1971) Reversible dissociation of carbamyl phosphate synthetase into a regulated synthesis subunit and a subunit required for glutamine utilization. *Proc Natl Acad Sci U S A 68*, 2599–2603.

(59) Mareya, S. M., and Raushel, F. M. (1994) A molecular wedge for triggering the amidotransferase activity of carbamoyl phosphate synthetase. *Biochemistry 33*, 2945–2950.

(60) Mergeay, M., Gigot, D., Beckmann, J., Glansdorff, N., and Piérard, A. (1974) Physiology and genetics of carbamoylphosphate synthesis in Escherichia coli K12. *Mol Gen Genet 133*, 299–316.

(61) Rubino, S. D., Nyunoya, H., and Lusty, C. J. (1987) In vivo synthesis of carbamyl phosphate from NH3 by the large subunit of Escherichia coli carbamyl phosphate synthetase. *J Biol Chem 262*, 4382–4386.

(62) Gigot, D., Crabeel, M., Feller, A., Charlier, D., Lissens, W., Glansdorff, N., and Pierard, A. (1980) Patterns of polarity in the Escherichia coli car AB gene cluster. *J Bacteriol 143*, 914–920.

(63) Raushel, F. M., Anderson, P. M., and Villafranca, J. J. (1978) Kinetic mechanism of Escherichia coli carbamoyl-phosphate synthetase. *Biochemistry 17*, 5587–5591.

(64) Thoden, J. B., Huang, X., Raushel, F. M., and Holden, H. M. (1999) The small subunit of carbamoyl phosphate synthetase: snapshots along the reaction pathway. *Biochemistry 38*, 16158–16166.

(65) Kim, J., and Raushel, F. M. (2001) Allosteric control of the oligomerization of carbamoyl phosphate synthetase from Escherichia coli. *Biochemistry 40*, 11030–11036.

(66) Thoden, J. B., Raushel, F. M., Wesenberg, G., and Holden, H. M. (1999) The binding of inosine monophosphate to Escherichia coli carbamoyl phosphate synthetase. *J Biol Chem 274*, 22502–22507.

(67) Thoden, J. B., Huang, X., Kim, J., Raushel, F. M., and Holden, H. M. (2004) Long-range allosteric transitions in carbamoyl phosphate synthetase. *Protein Sci 13*, 2398–2405.

(68) Anderson, P. M., and Meister, A. (1965) Evidence for an activated form of carbon dioxide in the reaction catalyzed by Escherichia coli carbamyl phosphate synthetase. *Biochemistry 4*, 2803–2809.

(69) Thoden, J. B., Wesenberg, G., Raushel, F. M., and Holden, H. M. (1999) Carbamoyl phosphate synthetase: closure of the B-domain as a result of nucleotide binding. *Biochemistry 38*, 2347–2357.

(70) Pierrat, O. A., and Raushel, F. M. (2002) A functional analysis of the allosteric nucleotide monophosphate binding site of carbamoyl phosphate synthetase. *Arch Biochem Biophys 400*, 34–42.

(71) Miles, B. W., Thoden, J. B., Holden, H. M., and Raushel, F. M. (2002) Inactivation of the amidotransferase activity of carbamoyl phosphate synthetase by the antibiotic acivicin. *J Biol Chem 277*, 4368–4373.

(72) Thoden, J. B., Huang, X., Raushel, F. M., and Holden, H. M. (2002) Carbamoyl-phosphate synthetase. Creation of an escape route for ammonia. *J Biol Chem 277*, 39722–39727.

(73) Fan, Y., Lund, L., Yang, L., Raushel, F. M., and Gao, Y.-Q. (2008) Mechanism for the transport of ammonia within carbamoyl phosphate synthetase determined by molecular dynamics simulations. *Biochemistry 47*, 2935–2944.

(74) Huang, X., and Raushel, F. M. (2000) An engineered blockage within the ammonia tunnel of carbamoyl phosphate synthetase prevents the use of glutamine as a substrate but not ammonia. *Biochemistry 39*, 3240–3247.

(75) Cook, P. F., and Cleland, W. W. (William W. (2007) Enzyme kinetics and mechanism (Rogers, R. L., Ed.) (alk. pape. Garland Science, London.

(76) Cleland, W. W. (1967) The statistical analysis of enzyme kinetic data. *Adv Enzym. Relat Areas Mol Biol 29*, 1–32.

(77) Miran, S. G., Chang, S. H., and Raushel, F. M. (1991) Role of the four conserved histidine residues in the amidotransferase domain of carbamoyl phosphate synthetase. *Biochemistry 30*, 7901–7907.

(78) Fan, Y., Lund, L., Shao, Q., Gao, Y. Q., and Raushel, F. M. (2009) A combined theoretical and experimental study of the ammonia tunnel in carbamoyl phosphate synthetase. *J Am Chem Soc 131*, 10211–10219.

(79) Kim, J., and Raushel, F. M. (2004) Perforation of the tunnel wall in carbamoyl phosphate synthetase derails the passage of ammonia between sequential active sites. *Biochemistry 43*, 5334–5340.

(80) Trotta, P. P., Burt, M. E., Haschemeyer, R. H., and Meister, A. (1971) Reversible dissociation of carbamyl phosphate synthetase into a regulated synthesis subunit and a subunit required for glutamine utilization. *Proc Natl Acad Sci U S A 68*, 2599–2603.

(81) Holden, H. M., Thoden, J. B., and Raushel, F. M. (1999) Carbamoyl phosphate synthetase: an amazing biochemical odyssey from substrate to product. *Cell Mol Life Sci 56*, 507–522.

(82) Jones, M. E. (1980) Ellen Jones. *Ann. Rev. Biochem. 49*, 253–79.

(83) Evans, D. R., and Guy, H. I. (2004) Mammalian Pyrimidine Biosynthesis: Fresh Insights into an Ancient Pathway*.

(84) Anderson, P. M., and Meister, A. (1966) Control of Escherichia coli carbamyl phosphate synthetase by purine and pyrimidine nucleotides. *Biochemistry 5*, 3164–3169.

(85) Anderson, P. M., and Meister, A. (1966) Bicarbonate-dependent cleavage of adenosine triphosphate and other reactions catalyzed by Escherichia coli carbamyl phosphate synthetase. *Biochemistry 5*, 3157–3163.

(86) Raushel, F. M., Anderson, P. M., and Villafranca, J. J. (1978) Kinetic mechanism of Escherichia coli carbamoyl-phosphate synthetase. *Biochemistry 17*, 5587–5591.

(87) Trotta, P. P., Platzer, K. E., Haschemeyer, R. H., and Meister, A. (1974) Glutamine-binding subunit of glutamate synthase and partial reactions catalyzed by this glutamine amidotransferase. *Proc Natl Acad Sci U S A 71*, 4607–4611.

(88) Trotta, P. P., Estis, L. F., Meister, A., and Haschemeyer, R. H. (1974) Self-association and allosteric properties of glutamine-dependent carbamyl phosphate synthetase. Reversible dissociation to monomeric species. *J Biol Chem 249*, 482–489.

(89) Rubio, V., Cervera, J., Lusty, C. J., Bendala, E., and Britton, H. G. (1991) Domain structure of the large subunit of Escherichia coli carbamoyl phosphate synthetase. Location of the binding site for the allosteric inhibitor UMP in the COOH-terminal domain. *Biochemistry 30*, 1068–1075.

(90) Bueso, J., Lusty, C. J., and Rubio, V. (1994) Location of the binding site for the allosteric activator IMP in the COOH-terminal domain of Escherichia coli carbamyl phosphates synthetase. *Biochem Biophys Res Commun 203*, 1083–1089.

(91) Thoden, J. B., Raushel, F. M., Benning, M. M., Rayment, I., and Holden, H. M. (1999) The structure of carbamoyl phosphate synthetase determined to 2.1 A resolution. *Acta Crystallogr D Biol Crystallogr 55*, 8–24.